Doctoral Programme in Clinical Research
Faculty of Medicine
Helsinki University

NON-INVASIVE VASCULAR STRUCTURE AND PATHOLOGY USING VERY-HIGH RESOLUTION ULTRASOUND

Johnny Sundholm, MD

ACADEMIC DISSERTATION

To be publicly discussed in the Hattivatti Auditorium at the Children's Hospital with permission of the Faculty of Medicine of the University of Helsinki on October 11th, 2019 at 12 noon.

Helsinki 2019

ISBN 978-951-51-5424-8 (pbk.)
ISBN 978-951-51-5425-5 (PDF)

Unigrafia
Helsinki 2019

Supervisor:
Docent Taisto Sarkola, MD, PhD
Division of Cardiology, Children's Hospital
University of Helsinki, Helsinki University Hospital and Pediatric Research Center
Helsinki, Finland

Custos:
Professor Markku Heikinheimo, MD, PhD
Children's Hospital
University of Helsinki, Helsinki University Hospital and Pediatric Research Center
Helsinki, Finland

Reviewed by:
Professor Juhani Knuuti, MD, PhD
Turku PET Centre
University of Turku
Turku, Finland

Docent Heikki Valleala MD, PhD
Department of Rheumatology
University of Helsinki, Helsinki University Hospital, Helsinki, Finland

Discussed with:
Dr. Andreas Diamantopoulos MD, PhD, MPH
Department of Rheumatology
Martina Hansens Hospital
Oslo, Norway

Author information:

Johnny Sundholm, MD
Division of Cardiology, Children's Hospital
University of Helsinki, Helsinki University Hospital and
Pediatric Research Center
Stenbäckinkatu 9, POB 281, FIN-00029 HUS, Helsinki, Finland,
Phone: +358 50 4011154
Fax: +358947174706
E-mail: johnny.sundholm@helsinki.fi

The Faculty of Medicine uses the Urkund system (plagiarism recognition) to examine all doctoral dissertations.

“What is there in this world that truly makes living worthwhile?
Death thought about it.
- CATS, he said eventually. - CATS ARE NICE.”
-From Sourcery by Terry Pratchett

TABLE OF CONTENTS

ABBREVATIONS:

AMS	-	Arterial Measurement System
AT	-	Adventitia thickness
AUC	-	Area under curve
BA	-	Brachial artery
CCA	-	Common Carotid artery
CI95%	-	95% Confidence interval
CIMT	-	Carotid intima-media thickness
CV	-	Coefficient of variation
DA	-	Colour doppler
EC	-	Electronic caliper
EEL	-	External elastic lamina
FA	-	Femoral artery
GCA	-	Giant cell arteritis
HA	-	Halo
HDR	-	Halo-Doppler-ratio
HRU	-	High-resolution ultrasound
ICC	-	Intraclass correlation coefficient
IEL	-	Internal elastic lamina
ILA	-	Inflammation limited to the adventitia
IMAT	-	Intima-media-adventitia thickness
IMT	-	Intima-media thickness
IVUS	-	Intravascular ultrasound
IT	-	Intima thickness
LD	-	Lumen diameter

LHR-	-	Negative likelihood ratio
LHR+	-	Positive likelihood ratio
LOA	-	Limits of agreement
MT	-	Media thickness
RA	-	Radial artery
ROC	-	Receiver operating characteristic
SD	-	Standard deviation
TMI	-	Transmural inflammation
VHRU	-	Very-high resolution ultrasound

ORIGINAL PUBLICATIONS

This thesis is based on the following publications, referred to in the text by their Roman numerals.

I. Sundholm JKM, Gustavsson T, Sarkola T. Semi-automatic border detection software for the quantification of arterial lumen, intima-media and adventitia layer thickness with very-high resolution ultrasound. *Atherosclerosis* 2014 Jun;234(2):283-7

II. Sundholm JKM, Olander RF, Ojala TH, Andersson S, Sarkola T. Feasibility and precision of transcutaneous very-high resolution ultrasound for quantification of arterial structures in human neonates - comparison with conventional high-resolution vascular ultrasound imaging. *Atherosclerosis*. 2015 Apr;239(2):523-7

III. Sundholm JKM, Paetau A, Albäck A, Pettersson T, Sarkola T. Non-invasive vascular very-high resolution ultrasound to quantify artery intima layer thickness: validation of the four-line pattern. *Ultrasound in Medicine & Biology* 2019 Aug;45(8):2010-18

IV. Sundholm JKM, Pettersson T, Paetau A, Albäck A, Sarkola T. Diagnostic performance and utility of very-high resolution ultrasonography in diagnosing giant cell arteritis of the temporal artery. *Rheumatology Advances in Practice* 2019 Jul;3(2):rkz018

ABSTRACT

Very-high resolution ultrasound (VHRU, 25-55MHz) is a recently developed method for non-invasive assessment of vascular structures. With its increased ultrasound frequency, the method allows for noninvasive examination of the vascular wall *in vivo* with an axial resolution in the range of tens of micrometers. These characteristics make it a feasible method to determine vascular dimensions of superficial arteries and arteries in the pediatric population. This novel method has hitherto been validated for the assessment of arterial and venous wall layer thickness in children and young adults, but the opportunity to use border detection software to improve measurement characteristics, to assess vascular structures in preterm and term neonates, to assess intimal changes related with arterial aging, and to explore the clinical utility of the method in the assessment of inflammatory vascular disorders has not yet been investigated.

The aim of this thesis was the following: 1. Broaden the toolbox for VHRU image analysis, that is, to study the application of a semi-automatic border detection software to improve measurement characteristics of the arterial wall layers, 2. To assess accuracy, precision and feasibility of the VHRU method in assessing superficial arterial wall layers in preterm and term neonates, 3. To validate the VHRU method to assess age-related intimal thickening of the arterial wall, and 4. To determine the potential to implement the method as a noninvasive tool in the bedside diagnosis of giant-cell arteritis of the temporal artery in the outpatient clinic.

This Thesis shows that there is no significant difference in the technical precision or bias of arterial wall layer dimension measurements using a semi-automated border detection software compared to electronical calipers, but time of analysis is significantly shorter using the automated border detection software (71.5 ± 16.6s vs 156.6 ± 37.2s, $p<0.001$), and the software can, therefore, be used for the automation of arterial wall layer dimension measurements.

VHRU is feasible, accurate and precise in the measurement of arterial layer thickness (intima-media and intima-media-adventitia thickness) of proximal conduit arteries, such as carotid, brachial and femoral, in preterm and term neonates, whereas

conventional high-resolution ultrasound (HRU, <15 MHz) was limited by its resolution for this purpose. The resolution of VHRU is insufficient in the assessment of more peripheral conduit arteries such as the radial artery. The penetrance depth of VHRU is insufficient to assess the aorta.

VHRU is feasible and able to detect a thickened intimal layer, seen as a four-line pattern of the arterial far wall in the ultrasound image, in superficial peripheral muscular conduit arteries with intima thickness >0.06mm. Measurements leading-to-leading edge of the intimal layer are accurate compared with histological thickness (mean difference 0.007mm, 95% limits of agreement -0.042mm-0.057mm) and precise (coefficients of variation: intra-observer 15.7%, inter-observer 19.9%). The prevalence of intimal thickening increases with age. The validated method could potentially be used to monitor vascular health in the aging population.

VHRU is feasible, accurate and precise in assessing histological transmural inflammation related intimal thickening in patients with giant-cell arteritis of the temporal artery. The method was however not useful in patients with inflammation limited to the adventitia or without inflammation on histology. VHRU derived intima thickness >0.3mm is more specific and clinically more useful in the detection of transmural inflammation compared with the halo-Doppler sign obtained with conventional HRU (receiver operating characteristic, ROC area under curve 0.99, CI95% 0.97-1.00 vs. 0.75, CI95% 0.54-0.96, p=0.026). Intimal thickening is detectable for a longer period after start of glucocorticoid treatment compared with the halo-sign obtained with HRU.

In conclusion, very-high resolution ultrasound is an emerging method for the assessment of superficial vascular wall layer structures. The harmless and non-invasive method can detect near-microscopical changes in the vascular wall in human subjects from the newborn stage to old age. Very-high resolution ultrasound has a clinical potential in the non-invasive assessment of vascular health and disease related pathology.

INTRODUCTION

The development of ultrasonography has provided the possibility to non-invasively and without harm assess tissue structure and motion *in vivo*. Gradual equipment improvement of medical high-resolution ultrasound (HRU; 8-15 MHz) over time provided the opportunity to use ultrasound in the assessment of vascular structures in different populations.

In 1986 Pignoli et.al described in their landmark study how to reliably determine vascular wall dimensions using B-mode ultrasonography.(1,2) By comparing histologic slides of the carotid artery with images taken using B-mode ultrasound of the same artery, they were able to demonstrate a double-line pattern in the ultrasound image of the elastic artery far wall. The first line was attributed to the ultrasound wave reflection at the blood to *tunica intima* -interphase, and the second reflection observed at the *tunica media* to *tunica adventitia* –interphase, with the distance between the interphases corresponding to the combined intima-media thickness (IMT).(3)

Sonographic measurements of the carotid intima-media thickness (CIMT) has since been adapted as a surrogate marker for subclinical early atherosclerosis and risk stratification of cardiovascular disease events including coronary artery disease, stroke, and peripheral artery disease in research settings.(4,5) The utility of CIMT-measurements for risk stratification in clinical settings has recently been disputed, and it has, as a consequence, been removed from the latest clinical guidelines.(6,7)

In 2010 Sarkola et al. described the use of very-high resolution ultrasound (VHRU; 25-55 MHz) for the analysis of the vascular wall layers in smaller muscular conduit arteries. The ultrasound frequency related improved resolution allowed arteries to be examined in more detail. A triple line pattern in the ultrasound image was described with the separate and simultaneous quantification of the far wall combined intima-media (IMT) and adventitia (AT) thickness. The measured thickness of the first reflection grossly overestimated the thin healthy intima layer thickness (IT) in animal specimens.(6) The increased resolution provided the opportunity to

image superficial muscular arteries IMT and AT not only in adults and adolescents, but in small children as well.(8)

This thesis further develops the VHRU method. It implements new tools for image analysis, evaluates the use of VHRU to assess the arterial wall structure in preterm and term neonatal populations, assesses the clinical utility of VHRU in bedside outpatient giant cell arteritis diagnosis, and further validates the method for the quantification of IT in the aging adult population.

1. LITERATURE REVIEW

1.1 PRINCIPLES OF ULTRASOUND IMAGING

Ultrasonography is based on the reflection of acoustic waves moving in tissue. Piezoelectric elements in the transducer converts electrical energy to pressure waves.(9) As the sound wave propagates in the tissue, it will interact with the tissue creating reflections that are recorded and processed.(10)

The acoustic impedance of tissue is the resistance of the tissue imposed on the propagating ultrasound beam. It is related to the density of the tissue influencing ultrasound propagation speed. The differences in impedance between different soft tissues is minute, whereas the acoustic impedance of bone is more than four times higher than that of soft tissue, and the acoustic impedance of air is immensely low resulting in diminished ultrasound reflections.

As the ultrasound beam reaches an interface of tissue with an increase in acoustic impedance, part of the acoustic wave will be reflected. The amount of reflected sound is directly related to the difference in acoustic impedance. Consequently, most of the ultrasound beam will be reflected at the border between soft tissue and bone. Both bone and air will thus limit imaging beyond the border.

Brightness mode (B-mode) ultrasound is based on the ultrasound waves reflected and detected by the transducer.(11) In B-mode imaging, differences in the intensity and transmission time of the reflected wave are translated into a 8 bit grey-scale image.

In optimal situations the tissue border is smooth and perpendicular to the ultrasound wave. In these occasions part of the wave will be reflected to the transducer and the rest will travel further through the tissue, i.e. specular reflection (Figure 1a). In the ultrasound image, the leading edge, defined as the surface of the bright reflection zone closer to the transducer, corresponds the true anatomical spatial tissue border. The leading edge is followed by a reflection trail ending in a trailing edge of the bright reflection zone. The thickness of the reflective trail, that is the distance between the leading and trailing edge, is independent of the thickness of the reflective tissue and is mainly related to ultrasound frequency and gain settings.

If the reflective interface is not completely smooth, part of the ultrasound beam will be scattered away from the transducer, reducing the intensity of the returning ultrasound wave, i.e. diffuse reflection (Figure 1b). If the ultrasound beam hits a surface with an angle that is not perpendicular to the soundwave, the reflection will divert away from the transducer, i.e. refracted, reducing image quality (Figure 1c). The ultrasound beam will further interact with small structures causing the ultrasound beam to scatter in all directions (Figure 1d).

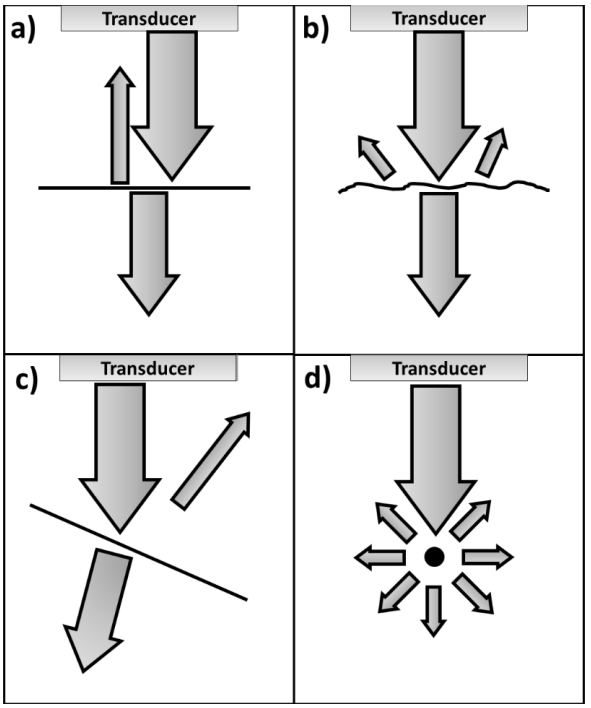

Figure 1. *Different kinds of ultrasound reflection: a) specular reflection, b) diffuse reflection, c) refraction, and d) scattering.*

Image resolution and imaging depth are important factors to consider when imaging vascular structures, and both are related with ultrasound frequency.(12) Whereas the resolution increases with frequency, the imaging depth or the penetrance is reduced. The main categories of resolution are the following (Figure 2a):

1. Temporal resolution, the smallest time interval at which two different events can be separately distinguished. A high temporal resolution is important when measuring movement of e.g. the arterial wall or the heart. The temporal resolution is related to the transmission time, and therefore the imaging depth, and the number of scan lines.

2. Axial resolution is the ability to spatially distinguish two points in the depth of the image. The axial resolution is of great importance when assessing different layers of the vascular wall with ultrasound. It corresponds directly to the wavelength and, thus, the frequency of the transducer as follows:

$$d = \lambda/2$$

Where d is the axial resolution, and λ is the wavelength. The wavelength is related to the propagation speed in tissue (*c*, on average 1540m/s in soft tissue) and the frequency, *f*, as follows:

$$\lambda = c/f$$

And the axial resolution:

$$d = c/2f$$

Higher frequencies then provide a smaller pixel size in the axial direction and improved resolution (Figure 3a).(13)

3. Lateral resolution is the ability to distinguish two points in the plane of the transducer. The lateral resolution is dependent on the beam width, that is related to width of the apparatus, the wavelength, and the depth. The lateral resolution varies across the image and is highest at the focal point after which it diminishes.

4. Out-of-plane resolution or slice thickness resolution is the ability to distinguish the plane from surrounding areas, i.e. the thickness of the field of view. The out-of-plane resolution is usually similar to the lateral resolution and is important when imaging small arterial structures bordering the resolution limit (Figure 2b).(14)

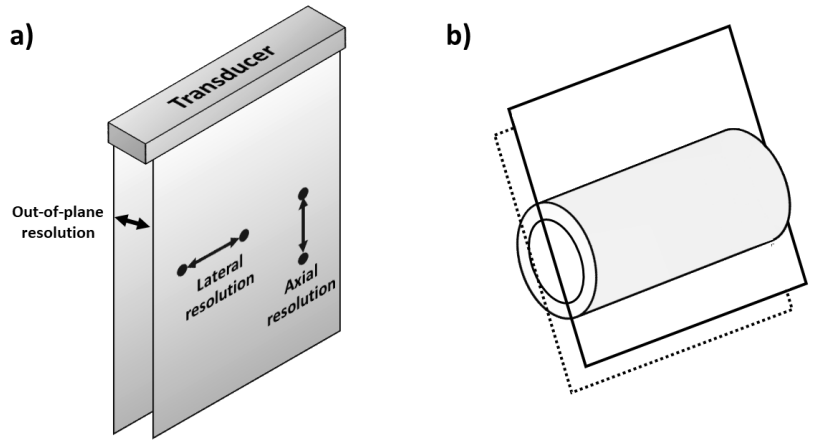

***Figure 2**. Schematic images a) of different spatial resolutions of ultrasound, and b) how the different resolutions affect imaging of vascular structures in the transverse plane. The axial resolution determines if two independent layers can be separately viewed, whereas insufficient out-of-plane resolution may distort the image leading to inexact measurements.*

Imaging depth, the penetrance, of ultrasound is influenced by the output intensity of the ultrasound beam and the attenuation of ultrasound in tissue. Attenuation is the rate at which the ultrasound beam weakens when passing through tissue. When the sound wave propagates in the tissue, part of the energy from the wave will be absorbed by the tissue and converted to heat, part will be reflected at tissue interfaces and part will be diverged away from the transducer.(9)

The gradual absorption of energy increases for shorter wavelengths and higher ultrasound frequencies. As the output intensity is relatively constant between devices, the penetrance depth is mainly related to tissue density and inversely related to ultrasound frequency.(15) The penetrance depth in soft tissue of typical ultrasound systems can be calculated as approximately:

$$D_{max} = 400 \times \lambda \text{ or } D_{max} = 400 \times c/f$$

Where D_{max} is the maximal penetrance distance of the ultrasound system, λ is the wavelength, c is the propagation speed in tissue, and f is the frequency of the transducer (Figure 3b).(13,16)

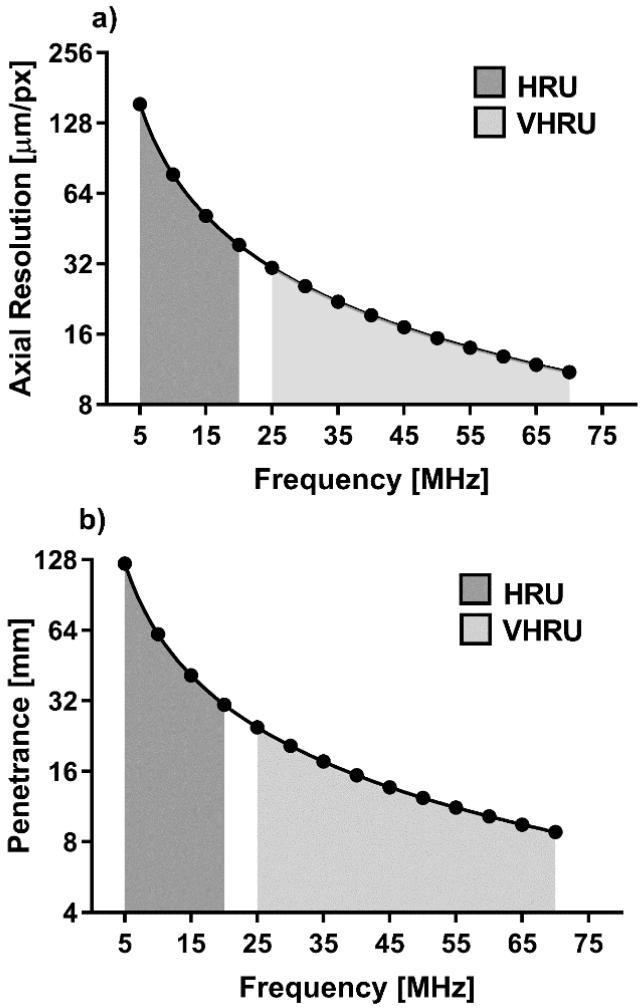

Figure 3. *The relationship of a) ultrasound transducer frequency and axial resolution and b) ultrasound transducer frequency and penetrance for high-resolution ultrasound (HRU) and very-high resolution ultrasound (VHRU).*

The choice of transducer is, thus, a balance between penetrance and resolution.(17) The frequency should be low enough to allow sufficient penetrance, but high enough to optimize image resolution. In a clinical setting, the frequency range of ultrasound is typically 2-20 MHz, with the lower frequencies mainly used for scanning of deeper targets such as organs in the abdominal cavity.(11) Smaller and superficial structures including blood vessels require a higher frequency to be appropriately assessed in the near field. Still, the highest frequencies currently applied in a clinical setting (15-20MHz) are limited by the axial resolution when imaging peripheral smaller muscular conduit arteries and arteries in small children.(18)

1.2 ARTERIAL AGING

The large and medium sized arteries are divided into categories of elastic and muscular arteries differing by size and histology. The elastic arteries are the arteries most proximal to the heart, such as the aorta, subclavian, carotid and iliac arteries. The muscular conduit arteries are smaller and distal to the elastic arteries. Most of the further named arteries, such as the brachial, femoral and radial arteries are muscular arteries.(19)

The arterial wall of large and medium sized arteries is divided into three layers: the intima, the media, and the adventitia, each separated by two elastic laminae (Figure 4a and 4b).(20,21) The intima consists of a layer of endothelial cells supported by a layer of elastic tissue (internal elastic lamina, IEL). In healthy arteries, the intimal thickness is very thin, often difficult to quantify and measuring 10-30 µm on histological sections.

The media is the thickest layer of the arterial wall with a thickness ranging from 600-1000 µm for the aorta and 50-150 µm for smaller muscular arteries, such as the radial and coronary arteries.(8,22) In elastic arteries the media consist of smooth muscle cells and circumferential elastic fibers, whereas the media of muscular arteries consists predominantly of smooth muscle cells.(20)

The outermost elastic layer of the media is called the external elastic lamina (EEL), underneath which lies the adventitia. The structure of the adventitia varies between

arteries and locations and consist generally of an inner compact and an outer loose layer of elastic fibers and connective tissue.(23)

Arterial aging starts during childhood.(24-30) Throughout life the arterial wall will be exposed to shear stress, oxidative stress and inflammation leading to endothelial dysfunction and remodeling of the arteria wall. There will be increased amounts of collagenous fibers and a reduction in smooth muscle cells and elastic fibers, with fragmentation of the elastic laminae resulting in increased arterial stiffness.(31-37)

Smooth muscle cells will further migrate to the intimal layer causing diffuse intimal thickening (Figure 4c).(38-41) Diffuse intimal thickening is seen as an adaptive physiological process in vascular ageing and not considered part of the atherogenic process.(42) Evidence, however, suggest that there's a link between cardiovascular morbidity and diffuse intimal thickening, and that intimal thickening is more abundant in atherosclerosis prone regions.(43,44) One suggested mechanism is that diffuse thickening of the intima damages the endothelium increasing its permeability for lipids. It will, thus, allow for lipid accumulation in the vascular wall. A lipid-driven inflammation will further lead to plaque formation and calcification (Figure 4d).(45-49)

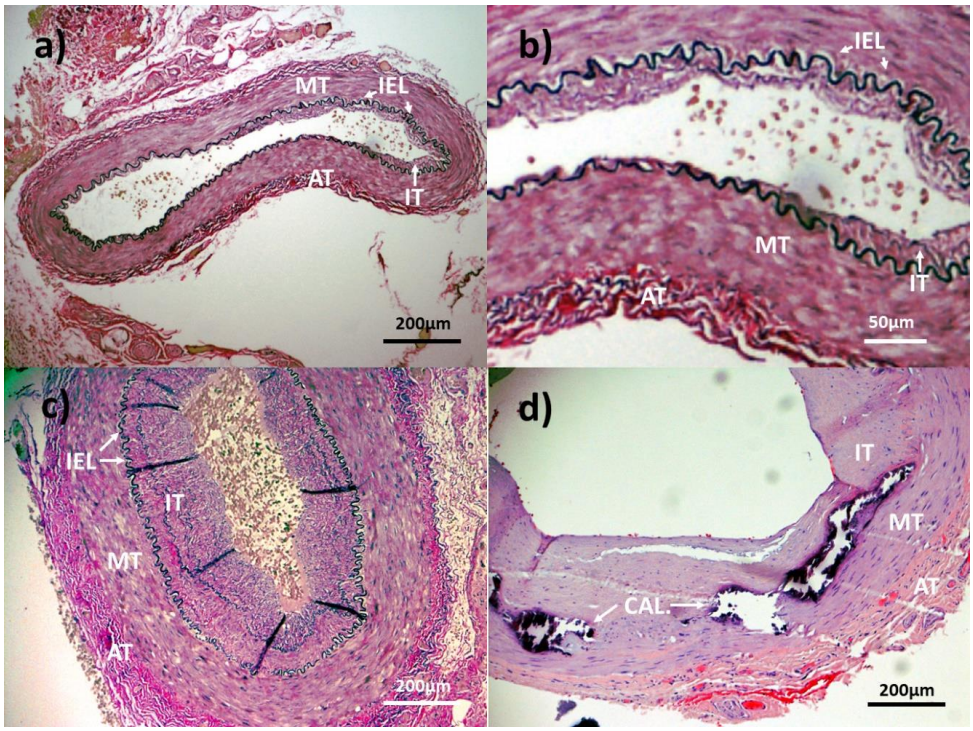

Figure 4. *Histology of a) and b) a temporal artery without evident intimal thickening or remodeling of the vascular wall, c) a temporal artery with diffuse intimal thickening, and d) a temporal artery with diffuse intimal thickening and focal calcification of the vascular wall. AT – adventitia; CAL – Calcification; IEL – Internal Elastic Laminae; IT – Intima; MT – Media.*

1.3 ASSESSMENT OF THE ARTERIAL WALL USING ULTRASOUND

As the ultrasound waves travel through the vascular wall it will cause a reflection at the interface of two mediums of different acoustic impedance. The leading edge corresponds to the true tissue border, whereas the trailing-edge reflects scatter in tissue related to transducer frequency and gain setting.

The acoustic impedance changes with the histological layers of the arterial wall and will thus cause echogenic reflections at the borders with intermediate echolucent regions. If the resolution is sufficient, there will be four reflective regions in the arterial wall, whereas insufficient resolution will cause fusion of the regions in the ultrasound image.

The first reflection appears at the lumen-intima interface as the acoustic impedance increases from blood to intima wall tissue (Z1). The second reflective region is at the internal elastic lamina between the intima and the media as elastin has a higher acoustic impedance than the surrounding layers (Z3). The third reflection is similarly at the external elastic lamina between the media and the adventitia (Z5). The last reflection appears at the edge between the adventitia and the perivascular tissue (Z7).(3,50,51) The intermediate zones Z2, Z4, and Z6 are variably echolucent regions without ultrasound reflection. Arterial wall layer thickness measurements with ultrasound are based on the distance between different reflective zones. These seven echo zones of the arterial wall (Z1-7) are schematically presented in Figure 5 and will be referred to throughout this thesis.

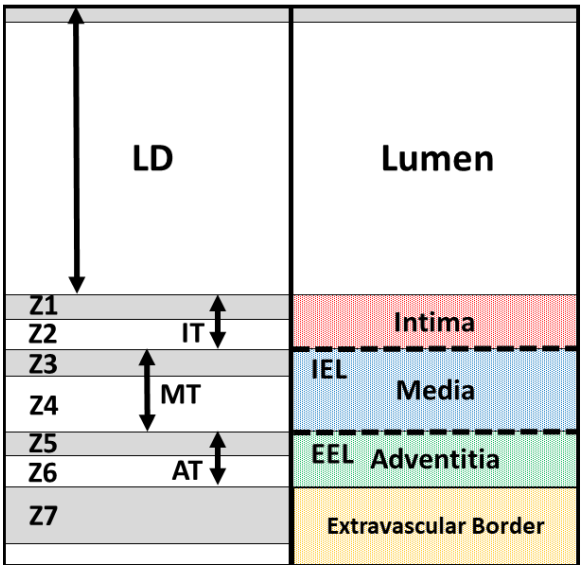

Figure 5. *Schematic image of the different reflective zones and their histological counterparts of the arterial wall. Z1- Zone 1, reflection at the border of the vascular lumen and the intima; Z2 – Zone 2, echolucent intima zone; Z3 – Zone 3, reflection from the internal elastic lamina; Z4 – Zone 4, echolucent media zone; Z5 – Zone 5, reflection from the external elastic lamina; Z6 – Zone 6, echolucent adventitia zone; Z7 – Zone 7, reflection from the adventitia and vascular wall border. Note that the histological borders correlate with the leading edge of the reflection. AT – Adventitia thickness; EEL – External elastic lamina; IEL – Internal elastic lamina; IT – Intima thickness; LD – Lumen diameter; MT – Media thickness.*

In 1986 Pignoli et al. first published their research on carotid artery ultrasound and described the double line pattern seen in the carotid artery far wall. It was shown to correspond to the intima-media thickness (IMT) of the artery (Figure 6). (1,2) The results were further confirmed by multiple independent groups stressing the importance of measurements performed at the far wall (rather than the near wall) and using the leading-to-leading edge technique. (52-54)

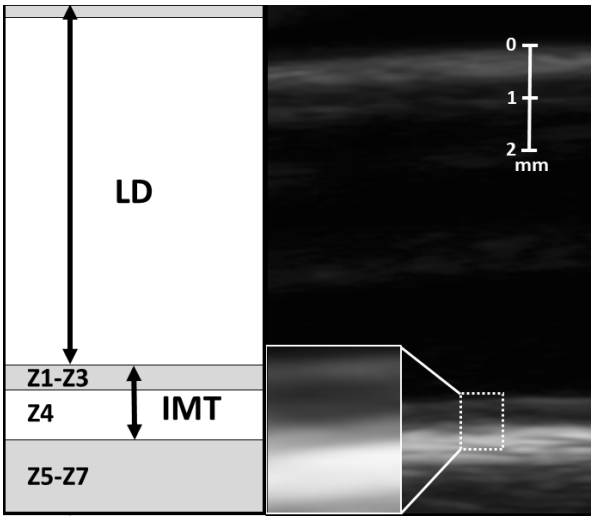

***Figure 6**. Schematic and ultrasound images of a carotid artery using a 25MHz transducer. Note how the intima and adventitia are not distinguishable and the echo zones Z1-3 and Z5-7 are fused. IMT – Intima-media thickness; LD – Lumen dimension. Modified from Sundholm et.al. 2019 (III).*

Carotid artery intima-media thickness (CIMT) has since then been confirmed as an independent predictor of cardiovascular disease including stroke and is widely used as a surrogate marker for cardiovascular disease in research settings.(55-62) The relevance of CIMT measurements in clinical settings has lately been disputed, as the evidence of added prognostic values is contradictory. Some studies suggest that there is no evident increase in prognostic value compared to traditional risk scores, e.g. the Framingham score.(63,64) As a result CIMT measurements are no longer recommended in the latest clinical guidelines.(6,7)

The limitations of the methods are suggested to be related to a non-pathological age related increase in CIMT, whether measurements are done in the common or internal carotid areas, inclusions of plaques, and inevitable technical variation in the measurement.(65,66)

These limitations increase the need for rigid and standardized measurement protocols and minimization of technical variance e.g. using automated measurement systems and comparing measurements with references for age.(66-68)

1.4 VERY-HIGH RESOLUTION ULTRASOUND

The use of very-high resolution ultrasound (VHRU, 25-55MHz) has during the last decade been adopted in the assessment of vascular morphology *in vivo*.(18,69) It was primarily developed for preclinical use and mainly to investigate anatomy and pathology of organs in small mammals.(70,71) The higher frequencies of this method allow the visualization of the vascular wall structure in almost microscopical detail (axial resolution 0.015-0.033mm), and limited mainly by its penetrance (as seen in Figure 3), allowing imaging of superficial peripheral conduit arteries and vascular imaging in small children.(8,18)

VHRU derived measurements of peripheral artery IMT has been shown to be applicable in different populations and study settings, and has been suggested as a surrogate marker for cardiovascular disease similar to CIMT.(72-77) VHRU has further been shown to be beneficial when assessing vascular wall damage as a sequalae to intravascular and surgical interventions and as an aid for vascular access and cannulation.(78-82)

Different non-invasive ultrasound derived estimations of the adventitia thickness (AT) of the carotid artery has previously been attempted using HRU. The total arterial wall thickness was defined by Hodges et. al. as the distance from the far wall arterial lumen to the trailing edge of the echogenic zone surrounding the IMT (Z5-7) showing great repeatability but without histological verification.(83) Skilton et al. introduced the concept of extra media thickness. They measured the distance from the leading edge of the echogenic zone at the lumen - far wall interface of the jugular vein to the trailing edge of the adventitia to media transition area (EEL) of the common carotid near wall. The extra media thickness method was reported to reflect carotid artery AT, but inevitably included perivascular tissue. The method was introduced without histological verification.(84,85) Since then a handful of studies have assessed the relation of extra media thickness with cardiovascular disease.(86-88) These methods are, however, limited by lack of proper validation.

Early *in vitro* validation of the VHRU method on animal arterial specimen showed a distinct triple line pattern in muscular arteries with the method reported as an

extension to the traditional double-line pattern method originally validated for the carotid artery IMT assessment (Figure 7a). Leading-to-leading edge measurements of the separated Z5-Z7 in the triple line ultrasound image corresponded to the histological AT. A similar pattern was, however, not seen in elastic arteries, and this was speculated to be related to differences in the composition of the adventitia in the different artery types. (18)

The increased resolution of VHRU frequencies and experiences of intima layer assessments using intravascular ultrasound (IVUS) also generated an interest of applying non-invasive VHRU for the assessment of superficial conduit artery IT. In 2001 Rodriguez-Macias et.al. reported on a method assessing IT measuring the leading-to-trailing edge distance of the first echogenic zone of the artery far wall with a 25MHz transducer. The authors concluded that the ultrasound-derived IT overestimated the histological IT.(89) The VHRU-IT method was later in 2007 validated by Osika et al with 55 MHz, using silicone phantoms and mesenteric arteries with evident intimal thickening (100-400µm), but without histological validation in the peripheral muscular conduit artery IT range (<100 µm).(69) Since then the leading-to-trailing edge method has been further evaluated, and its use as a surrogate marker for cardiovascular disease has been assessed in multiple studies.(90-99) The interpretation of these results is difficult due to the controversial validation of the method based on a leading-to-trailing edge principle.

The leading-to-trailing edge method has been disputed, as the accuracy of the trailing edge border is influenced by ultrasound scatter, and the thickness of the ultrasound reflection is independent of the thickness of the structure generating the reflection. (3,68) Sarkola et.al. compared VHRU measurements of IT obtained with the leading-to-trailing edge method, as suggested by Osika et al (70), with histology IT in healthy animal arterial specimens. They found that the VHRU derived IT grossly overestimated histological IT and showed no correlation with histological IT. They concluded that the variability observed in the VHRU IT measurement of the healthy artery using the Osika method is due to technical variability in the VHRU leading-to trailing edge measurement (i.e. background noise), and that the healthy artery IT is

below the axial resolution limit and, thus, beyond the resolution of VHRU frequencies.(18)

Vatanen et.al. recently described a distinct four-line pattern of the arterial far wall obtained with VHRU among long-term child cancer survivors that was related with radiotherapy in early childhood. The four-line pattern allowed IT measurements leading-to-leading edge within the near blood intima region, and this was interpreted to represent diffuse intimal thickening allowing ultrasound quantification of IT. However, their measurements were reported without histological verification (Figure 7b).(100)

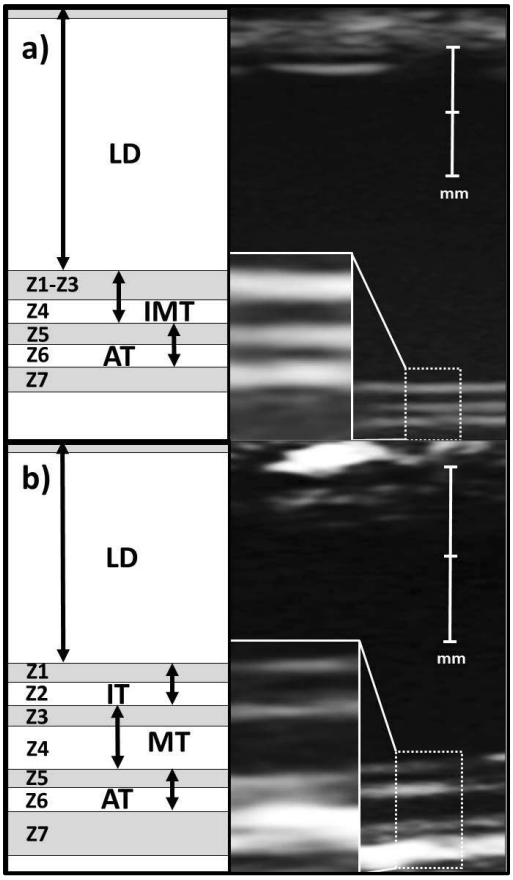

Figure 7. *Schematic and ultrasound images (55MHz) of radial arteries with a) no intimal thickening, showing the triple-line pattern, note how the intima is beyond the axial resolution and zones Z1-3 are fused, and b) intimal thickening seen as a four-line pattern with seven distinct echo zones (Z1-Z7). The scale bar represents 1mm. LD – Lumen dimension IT – Intima thickness; IMT – Intima-media thickness; MT – Media thickness; AT – Adventitia thickness. Modified from Sundholm et.al. 2019 (III).*

1.5 BORDER DETECTION SOFTWARE

Measurements of arterial wall dimensions using manual electronical calipers (EC) are time consuming and prone to technical variation due to interobserver variability in image interpretation.(68,101) The development of semi-automated and later fully automated border detections software were initiated to address these issues.(3,102,103)

There are now multiple software available that use different algorithms to identify the borders of the lumen and the vascular wall, either with the aid of human supervision or fully automated.(102-109) The commercially available systems are developed for HRU systems and do not currently support measurements of intima or adventitia thickness. The software is limited mainly to CIMT and plaque identification and have not been validated for analysis of VHRU images.

The main benefits of border detection software include less interobserver dependence and variability over time avoiding measurement drift. The semi-automated systems still slightly outperform the fully automated systems(101,110,111), and their use are recommended by current guidelines.(7,67,112) The software currently available are, however, validated for IMT and plaque measurements only.

1.6 ULTRASOUND DIAGNOSTICS OF GCA

1.6.1 GIANT CELL ARTERITIS OF THE TEMPORAL ARTERY

Giant cell arteritis (GCA) is an inflammatory vasculopathy affecting predominantly medium and large size vessels that has a well-defined adventitial vasa vasorum.(113-115) It is the most common primary vasculitis with a global incidence of 10/100 000 and an even higher incidence in northern Europe (20/100 000).(116-119) The peak incidence is between ages 70 and 80 years, and the disease is rarely seen among individuals younger than 50 years old. 65-75% of affected individuals are women, and there is a 50% comorbidity with polymyalgia rheumatica.(119-121)

The inflammation in GCA is to be derived from activation of dendritic cells in the *vasa vasorum* around the vascular wall.(122,123) The activated dendritic cells infiltrate

the vascular wall recruiting CD4+ T-cells and macrophages causing inflammation.(124) There is an increased matrix metalloproteinase activation and smooth muscle cell migration to the intima causing destruction of the elastic laminae and intimal hyperplasia.(125-127) The intimal hyperplasia can cause lumen occlusion and ischemic complications distal to the inflammation. Visual loss is the most feared ischemic complication seen in around 15% of untreated patients.(128,129)

The golden standard for GCA diagnosis is biopsy of the temporal artery showing marked inflammation of the vascular wall.(130-132) The biopsy is, however, not flawless. The inflammation may be segmental causing false-negatives. The sensitivity ranges from 32-90%, with reduced sensitivity in patients with predominantly extra-cranial large vessel vasculitis and/or prolonged glucocorticoid treatment.(133-140) Biopsy of the temporal artery is further an expensive and invasive procedure and, even though complications are scarce, it is not risk free. Furthermore, it is not applicable for follow-up assessments.(141-143)

1.6.2 THE HALO-SIGN IN HIGH-RESOLUTION ULTRASOUND

In 1997 Schmidt et al. described a hypodense perivascular halo sign in the temporal artery of patients with GCA using colour Doppler HRU (Figure 8).(144) The halo-sign was described to represent the oedematous and thickened vascular wall. Thus, grew the interest to refine this non-invasive tool for GCA diagnostics.(145-158)

The halo-sign was shown to be specific and sensitive in the setting of transmural inflammation, with a sensitivity of 68-75% and a specificity of 83-91% for an unilateral halo sign and a specificity of 100% for a bilateral halo sign with slight reduction in sensitivity (46%), confirmed by meta-analyses.(159-163)

A major drawback of the method is significant loss of sensitivity after only 2-4 days glucocorticoid treatment.(164) A further limitation is the operator dependency and subjectivity of the interpretation leading to variable results. There has been a call for standardization of imaging protocols to refine the diagnostic process.(165,166) For instance, cut-off values for diagnosis have been reported to reduce the rate of false positives.(157,167,168).

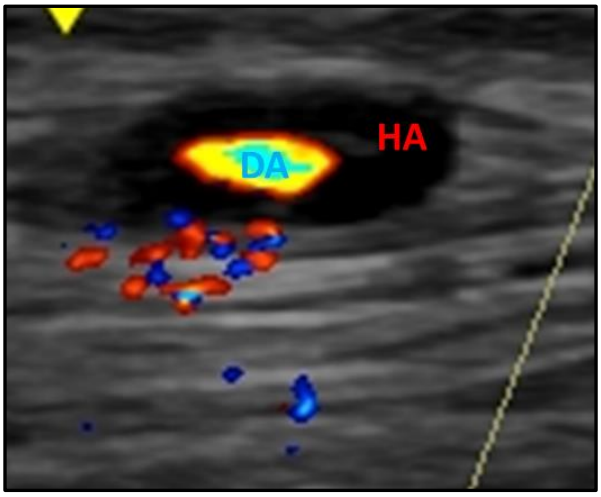

Figure 8. *The perivascular halo-sign diagnostic for giant-cell arteritis as seen with a 15MHz transducer. DA – Colour Doppler representing the blood flow of the lumen; HA – a dark halo surrounding the lumen, representing an oedematous, thickened vascular wall. Modified from Sundholm et.al. 2019 (IV).*

The method is robust and the halo sign has been included in the latest EULAR recommendations for diagnostic criteria of GCA as an alternative to temporal artery biopsy.(169-172) So far only a handful of studies has assessed the utility of VHRU for the assessment of temporal artery morphology in GCA in small samples and without diagnostic utility assessment, or comparison to HRU. (173-176)

2. OBJECTIVES

I. To assess the feasibility of a semi-automatic border detection software on very-high resolution ultrasound images and explore benefits regarding analysis time and precision compared with manual electronic calipers.

II. To study the feasibility, accuracy and precision of non-invasive very-high resolution ultrasound to assess arterial wall morphology in preterm and term neonates in vivo, and to compare the method with conventional high-resolution ultrasound.

III. To validate the very-high resolution ultrasound derived four-line pattern, in comparison to histology, as a method to quantify arterial intima thickness non-invasively *in vivo*.

IV. To study the clinical diagnostic utility of very-high resolution ultrasound in comparison with conventional high-resolution ultrasound in the assessment of temporal artery manifestations of giant cell arteritis.

3. METHODS

3.1 RESEARCH SETTING AND STUDY DESIGN

This study was carried out at the Children's Hospital, Helsinki University Hospital, between 2011 and 2018. All studies are prospectively recruited cross-sectional studies.

3.2 ETHICS

The local research ethics board approved the study and written informed consent was obtained from patients and from parents of minors. Permission to use the Vevo 770 equipment (Visualsonics, Toronto) for studies on human subjects was obtained from the Finnish National Supervisory Authority for Welfare and Health, Valvira.

3.3 STUDY POPULATIONS

3.3.1 STUDY I

The study population of study I consisted of 10 healthy subjects of both sexes, including both adults and children (age range 5-56 years). The population was investigated at two occasions two weeks apart between December 2011 and January 2012. Exclusion criteria were previously diagnosed cardiovascular disease and previous surgical or intravascular interventions to carotid, brachial, radial, femoral or posterior tibial arteries assessed in the study.

3.3.2 STUDY II

The study population consisted of 25 neonates of different gestational ages (range from 33+0 to 41+5 weeks) and weights (range from 1570 to 4950 gram) recruited between November 2011 and January 2014 within 3 days of delivery at the Women's Hospital, Helsinki University Hospital. Subjects with cardiac or extra cardiac malformations, or medication affecting the cardiovascular system during the antenatal or postnatal periods were excluded.

3.3.3 STUDY III AND IV

For study III and IV we recruited 74 (study III) and 78 patients (study IV) with suspected giant cell arteritis (ages 40-86 years) referred to the unit of Vascular

Surgery at Helsinki University Hospital for biopsy of the temporal artery between August 2015 and May 2018.

Study III and IV excluded subjects with failed biopsy (N=3). Study III further excluded all patients with any sign of inflammation on temporal artery biopsy (N=20), biopsies sectioned diagonally precluding reliable assessment of vascular dimensions on histology (N=8), and patients missing vascular VHRU images of sufficient resolution due to equipment breakdown (N=6), with 37 subjects included in the final analysis.

Study III further included a convenience sample (N=380) recruited in other previous or current ongoing longitudinal research projects consisting of 1. young healthy children and adolescents (age 0-18 yrs., n=139 (8)), 2. teenagers with type 1 diabetes (age 13-16 yrs., n=39, unpublished), 3. healthy males (age 20-46 yrs., n=24, unpublished), and 4. a sample of women with obesity and or gestational diabetes (age 28-51 yrs., n=178, unpublished).

3.4 ULTRASOUND EQUIPMENT AND IMAGE ANALYSIS SOFTWARE

3.4.1 VERY-HIGH RESOLUTION ULTRASOUND SYSTEMS (VHRU)

Very-high resolution images were obtained using Vevo 770 (VisualSonics, Toronto, Canada, 2005) for study I-II and for the first 41 subjects of study III-IV, and using Vevo MD (VisualSonics, Toronto, Canada, 2016) for the remaining subjects in study III-IV. The technical details of the VHRU devices and their transducers are shown in Table 1.

3.4.2 CONVENTIONAL HIGH-RESOLUTION ULTRASOUND (HRU)

Conventional HRU systems in this study were GE Vivid 7 (GE Healthcare, Chicago, IL, USA, 2001) equipped with 7 MHz and 12MHz transducers (study II), and for study IV, GE LOGIQ e (GE Healthcare, Chicago, IL, USA, 2015) equipped with a 18MHz vascular transducer for the first 41 subjects and the Vevo MD equipped with a 15MHz transducer for the rest.

Ultrasound System	**Vevo 770**	**Vevo MD**
Release Year	2005	2016
Transducer type	Single Mechanical	Multiple electrical
Image post-processing	None	Despeckling filter
Multi-focus	No	Yes
Transducers	**RMV710B**	**UHF22**
Centre transmit	25MHz	15MHz
Frequency range	12-38MHz	10-22MHz
Axial Resolution	70µm	100µm
Penetrance	22.5mm	38.4mm
Transducers	**RMV712**	**UHF48**
Centre transmit	35MHz	30MHz
Frequency range	17-53MHz	20-46MHz
Axial Resolution	50µm	50µm
Penetrance	13.0mm	23.5mm
Transducers	**RMV708**	**UHF70**
Centre transmit	55MHz	50MHz
Frequency range	22-83MHz	29-71MHz
Axial Resolution	30µm	30µm
Penetrance	8.0mm	10.0mm

Table 1. *Very-high resolution ultrasound systems and the transducers used in this study. From the supplemental material of Sundholm et.al. 2019 (III), used with permission from Elsevier*

3.4.3 IMAGING PROTOCOL

All images were obtained at rest in supine position. Care was taken not to compress the artery and the highest frequency allowing visibility of the far wall was used. Images were recorded perpendicular to the vascular wall, with gain settings and focal depth adjusted to reduce scatter, and to optimize image quality.

Images of the carotid artery for measurements of vascular dimension were processed according to guidelines(4) 1 cm proximal to the bulb (study I-III) and the arteries were further screened for plaques throughout the bulb and bifurcation as

far as visibility allowed (study III). The radial artery was imaged 1 cm proximal to the *palma manus* (study I and III), the brachial artery 2 cm proximal to the cubital skin fold (study I-III), the femoral artery at the inguinal skin fold (study I-II) and the posterior tibial artery at the level of the medial malleolus (study I). The temporal artery was screened from the zygoma arch distally throughout the common temporal artery (study III-IV), as well as the parietal and frontal branches after bifurcation. Images were stored as moving video clips and later analyzed offline.

3.4.4 IMAGE ANALYSIS SOFTWARE

VHRU images were analyzed using manual electronic calipers using vendor software Vevo 3.0.0 (Vevo 770) and VevoLab 2.0.0 (Vevo MD) (Study I-IV), and dimensions calculated as a mean of three measurements. In study I we further used a semi-automated border detection software (AMS, Arterial Measurement System (103) gustav@alumni.chalmers.se). GE Vivid 7 images were analyzed in AMS using electronic calipers, and GE LOGIQ e images using ImageJ 1.51J8 (National Institutes of Health, USA,(177)).

3.4.5 IMAGE ANALYSIS PROTOCOL

Vascular dimensions were measured from the far wall in end-diastole using the leading-to-leading edge method. Lumen diameter (LD) was defined as distance from the leading edge of the near wall intima-lumen interphase to the far wall leading edge of intimal-lumen interphase (Z1). Intima-thickness (IT) was measured from leading edge of Z1 to the leading edge of Z3. Intima-media thickness (IMT) was measured from leading edge of Z1 to leading edge of Z5. Intima-media-adventitia thickness (IMAT) was measured from leading edge of Z1 to leading edge of Z7. (Figure 5 & 9.) Adventitia thickness was calculated as the difference between IMAT and IMT. Image quality was subjectively graded into high or low quality according to visibility of the far wall in the ultrasound clip.

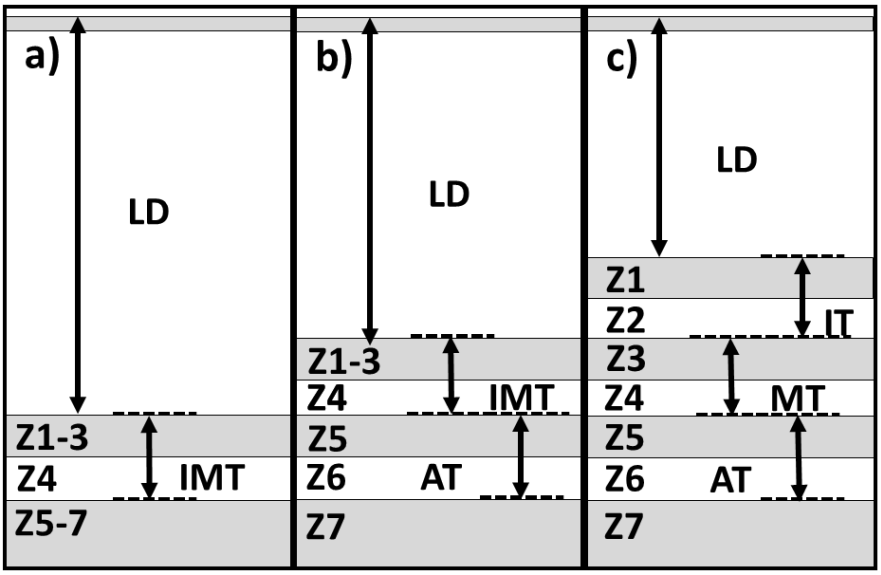

Figure 9. *Schematic images showing how leading-to-leading edge measurements of the far wall were performed, and corresponding dimensions in a) arteries with double-line pattern, b) arteries with triple-line pattern, and c) arteries with four-line pattern. Echo zones are defined in Figure 5 IT – Intima thickness; Intima-media thickness; MT – Media thickness; AT – Adventitia thickness; LD – Lumen dimension.*

Carotid arteries were evaluated for plaques (study III) according to the Mannheim consensus, defining a plaque as a focal thickening of IMT fulfilling one of the following criteria 1. IMT>1.5mm, 2. IMT increase of 0.5mm, or 3. >50% compared to the surrounding IMT. (67)

The perivascular Halo-sign in patients with suspected GCA was evaluated both subjectively and measured as a ratio of the perivascular halo area to Doppler lumen area as follows: HRU-HDR = Halo-area/doppler-area (Figure 10.)

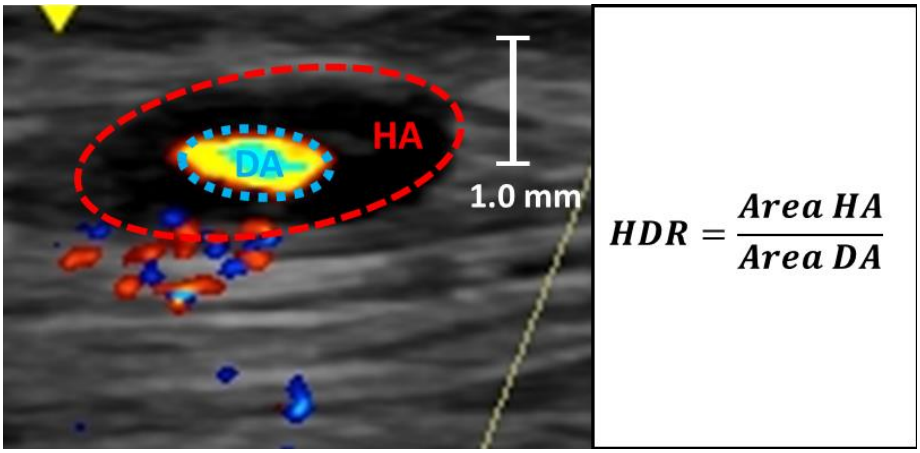

Figure 10. *Calculations of halo-doppler ratio from conventional high-resolution images. HDR – Halo-doppler ratio; HA – Halo-area; DA – Doppler area. Modified from Sundholm et.al. 2019 (IV).*

Intra-observer agreement was assessed by independently repeated analyses of the ultrasound clips performed by the primary investigator. For inter-observer agreement, the images were independently analysed by a second investigator. For test-retest variability (reproducibility), images of the same subject from two different imaging sessions were measured by the primary investigator (study I-II).

Measurement of Vevo images using AMS required extraction of a single image converted to lossless TIFF-format prior to analysis. Measurements were done in a 1-2cm wide region of interest automatically traced by the software. Manual correction of the traced borders was done only when deemed necessary by the operator. Analysis time was assessed for 20 individual clips using both electronical calipers and AMS (Study I).

3.4 HISTOLOGICAL PROCESSING

Biopsy of the temporal artery was done as routine diagnostics at Helsinki University Hospital Department of Vascular Surgery. The biopsy was fixed in formalin and cut in transverse sections (multiple levels) and stained with haematoxylin and eosin (H&E) and Verhoff's elastic stain (VEG).(178) Uncertain cases where further stained using T-lymphocyte CD3+ immunohistochemical stain.(179)

Biopsies were evaluated for vascular pathology at a certified pathology unit of the Helsinki University Hospital (HUSLAB). Histological assessments of vascular dimension were evaluated using optic microscopy (Nikon Eclipse 80i & Digital Sight DS-5M, Tokyo, Japan) photographed at 10x zoom, and vascular dimensions measured offline in ImageJ 1.51J8 using electronic calipers. Measures were calculated as the mean of 10 measurements to avoid focal variations in the vascular wall, with IT, IMT, and AT measured separately.

3.5 DIAGNOSTICS OF GIANT CELL ARTERITIS

Giant-cell arteritis diagnosis was determined on histological and clinical basis. The biopsy was deemed negative if there was no inflammation on histology (Figure 11a), or only mild inflammation limited to the perivascular area and/or the *vasa vasorum* as the significance of perivascular inflammation is controversial.(180) A biopsy with inflammation limited to the adventitia (ILA, Figure 11b) or transmural inflammation (TMI, Figure 11c and d) were defined as positive and diagnostic for GCA. Subjects with a negative biopsy were evaluated by an expert rheumatologist and final diagnosis was assessed on the basis of clinical findings, laboratory results, response to treatment, evidence of large vessel vasculitis on positron emission tomography (PET-CT) or magnetic resonance imaging (MRI), and a differential diagnostic work-up during a 6 month follow up from biopsy procedure. (181-189)

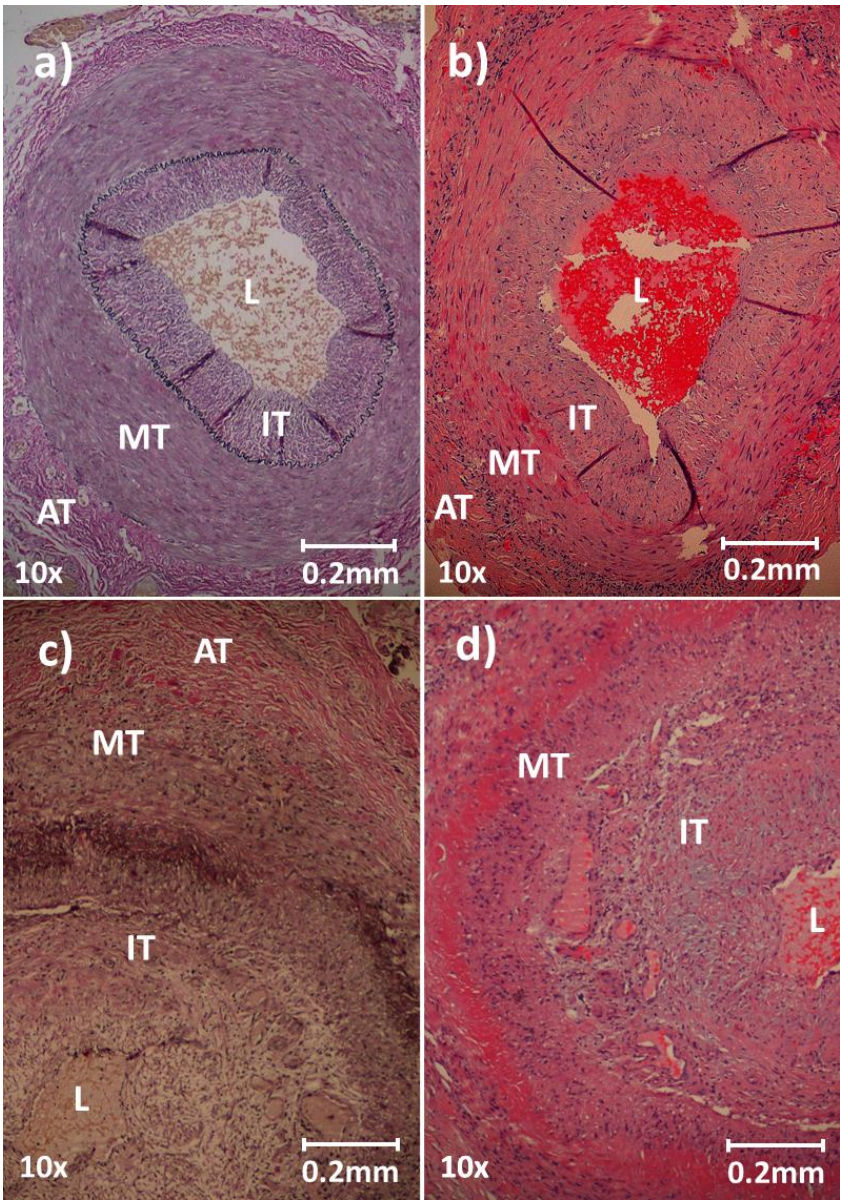

Figure 11. *Histology of Verhoff's elastic stain (A) of a temporal artery without inflammation ("No GCA" and "Clinical GCA without inflammation" groups). Histology of haematoxylin and eosin stain (B) of a temporal artery with minor inflammation limited to the adventitial layer (ILA). Note the streak of inflammatory cells throughout the media-adventitia border. Verhoff's elastic stain (C) and haematoxylin and eosin stain (D) of a temporal artery with transmural inflammation (TMI). AT – Adventitia; IT – Intima; L – Lumen; MT – Media. From Sundholm et.al. 2019 (IV).*

3.6 DATA ANALYSIS

Results are reported as mean with SD for continuous normally distributed variables, median and range for non-normally distributed continuous variables, and proportions for categorial variables. Shapiro-Wilk test was used to test normality.

Group comparisons were done using Student's T-test for continuous variables. Multiple groups were compared using ANOVA for normally distributed variables with post-hoc Bonferroni, Kruskal-Wallis for non-normally distributed continuous variables with post-hoc Dunn-Bonferroni, and Fisher-Freeman-Halton for categorial variables with post-hoc independent Fisher comparisons including Bonferroni adjusted levels of significance.

Agreement was quantified by calculating the mean difference, 95% limits of agreement (LOA), coefficient of variation (CV), and intraclass correlation coefficients (ICC), and further visualized using Bland-Altman plots.(190)

Multiple linear and logistic regression models were used to assess the relationship between scalar respectively dichotomous variables, and multiple explanatory variables.

Diagnostic performance was assessed using receiver operator characteristics-curves (ROC) and methods were compared using a paired test of equality for area under curve (AUC).(191) Cut-off values for different parameters were evaluated using sensitivity-specificity charts optimizing positive likelihood ratio (LHR+), and results reported using sensitivity, specificity, LHR+ and negative likelihood ratio (LHR-)

For all analyses a p-value of <0.05 was deemed statistically significant. Data analysis was performed using SPSS (IBM, NY, USA, study I-IV) and Stata MP (Stata corp., TX, USA, study III-IV).

4. RESULTS & DISCUSSION

4.1 STUDY I, AUTOMATED BORDER DETECTION SOFTWARE

One benefit of the semi-automated system was the shorter analysis time for a single image, with a reading time of 71.5 ± 16.6s for the semi-automated system (AMS) and 156.6 ± 37.2s for electronic calipers (EC) ($p<0.001$).

Intra- and interobserver as well as test-retest variabilities were similar for AMS and EC with no evident bias (Table 2-4, Figure 12). This is partly in disagreement with previous studies comparing manual measurements with semi-automated systems, where a systematic underestimation of IMT has been reported with semi-automated systems compared to manual caliper measurements, but with an improved technical measurement reliability.(192-195) This disagreement could be explained by a resolution mismatch with AMS primarily developed for lower resolution ultrasound images. Furthermore, the AMS software does not fully support VHRU image processing, which leads to increased manual interference.(103) This may have influenced measurement time as our analysis time for AMS was longer than previously reported for conventional ultrasound image processing.(108,196-198)

The lack of image preprocessing may also have influenced our results. We did not normalize image gray-scale or use despeckling filters which has been recommended by some to improve the border detection for automated systems.(199,200)

In a multiple linear regression model ($R^2 = 0.171$) the operator technical variability (CV%) was mainly predicted by 1. dimension size with increased relative variability for smaller dimension measurements (logarithmic relationship; $R^2 = 0.125$, $\beta = -4.800$, $p < 0.001$), 2. image quality ($R^2 = 0.015$, $B = -2.446$, $p < 0.001$), and 3. repeat imaging (test-retest) ($R^2 = 0.025$, $B = 2.669$, $p < 0.001$). There was no statistically significant effect of observer (inter-observer) or software ($R^2 = 0.002$, $p = 0.169$, and $R^2 = 0.000$, $p = 0.450$ respectively). Whereas dimension size has previously been shown to be related to increased relative variability, we did not find any earlier reports investigating the effect of image quality.(201)

We concluded that AMS as a semi-automated border detection software performs equally well compared to electronic calipers with significant shorter analysis time.

The main limitations of the study were the small sample size and inclusion of only healthy subjects with an age span not including infants or patients with marked cardiovascular disease. This precluded comparison of results between different age groups and effect of cardiovascular disease. Also, the assessment was performed with one software only. We did, however, include both children and adults, assessed the utility of AMS in multiple arterial locations, and included both elastic and muscular arteries in our study.

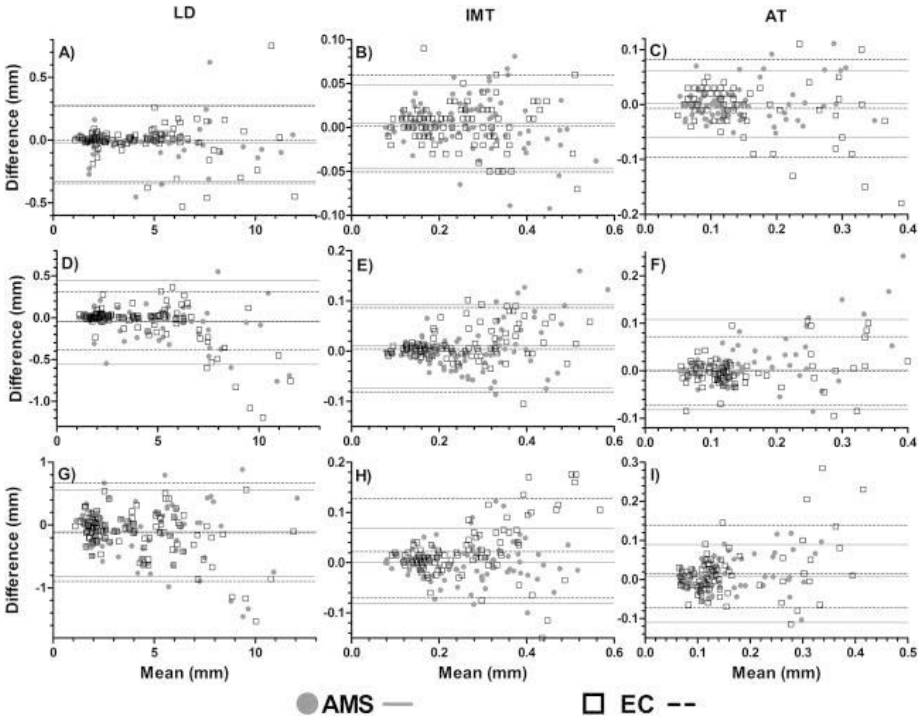

Figure 12. *Bland–Altman plots on semi-automated border detection software- (AMS) and electronic caliper-derived (EC) derived intra (A–C), inter (D–F), and test-retest (G–I) agreements for lumen dimension (LD), intima-media thickness (IMT) and adventitia thickness (AT) measurements. Mean difference and 95% limits of agreement are displayed with lines for both systems. From Sundholm et.al. 2014 (I), with permission from Elsevier.*

			Mean thickness [mm]		ΔMean (LOA 95%) [mm]		CV%		p-value
Artery	**Dimension**	**N**	**AMS**	**EC**	**AMS**	**EC**	**AMS**	**EC**	**AMS vs EC**
Carotid *25 MHz*	**LD**	20	5.601	5.559	0.010 (-0.036, 0.056)	0.034 (-0.177, 0.240)	0.4	1.9	0.033
	IMT	20	0.373	0.358	-0.006 (-0.072, 0.061)	-0.001 (-0.069, 0.067)	9.2	9.8	0.825
Femoral *25 MHz*	**LD**	20	7.751	7.849	-0.018 (-0.425, 0.388)	-0.062 (-0.636, 0.513)	2.7	3.7	0.270
	IMT	20	0.325	0.33	0.009 (-0.069, 0.087)	0.004 (-0.048, 0.055)	12.3	8.0	0.226
	IMAT	20	0.564	0.601	0.020 (-0.090, 0.130)	-0.025 (-0.189, 0.139)	10.0	14.0	0.397
	AT	20	0.239	0.271	0.010 (-0.083, 0.103)	-0.029 (-0.180, 0.123)	19.9	28.6	0.104
Brachial, Radial, Tibial 35-55MHz	**LD**	56	2.505	2.48	-0.008 (-0.087, 0.070)	-0.002 (-0.067, 0.071)	1.6	1.4	0.826
	IMT	59	0.182	0.179	0.007 (-0.021, 0.036)	0.001 (-0.030, 0.032)	8.0	8.8	0.597
	IMAT	58	0.291	0.285	0.003 (-0.036, 0.042)	0.003 (-0.044, 0.049)	6.8	8.3	0.197
	AT	60	0.108	0.106	-0.001 (-0.047, 0.045)	0.000 (-0.051, 0.051)	21.7	24.5	0.310

Table 2. *Intra-observer agreement of AMS and EC for different transducer frequencies, arterial sites and dimensions. LD – lumen dimension; IMT – intima-media thickness; IMAT – intima-media-adventitia thickness; AT – adventitia thickness; CV – coefficient of variation; ΔMean – mean difference; LOA 95% – 95% limits of agreement; AMS – semi-automatic border detection; EC – electronic calipers. From Sundholm et. al. 2014 (I), used with permission from Elsevier.*

Artery	Dimension	N	Mean thickness [mm]		ΔMean (LOA 95%) [mm]		CV%		p-value
			AMS	EC	AMS	EC	AMS	EC	AMS vs EC
Carotid *25 MHz*	**LD**	18	5.589	5.594	0.008 (-0.147, 0.163)	-0.030 (-0310, 0.249)	1.4	2.6	0.098
	IMT	20	0.398	0.382	-0.049 (-0.164, 0.067)	-0.047 (-0.116, 0.022)	14.8	9.2	0.065
Femoral *25 MHz*	**LD**	20	7.676	7.676	0.149 (-0.497, 0.795)	0.345 (-0.451, 1.140)	4.3	5.3	0.333
	IMT	19	0.316	0.322	0.019 (-0.065, 0.103)	0.003 (-0.063, 0.069)	13.5	10.4	0.109
	IMAT	19	0.577	0.600	-0.027 (-0.172, 0.119)	-0.015 (-0.095, 0.064)	12.9	6.8	0.001
	AT	19	0.261	0.278	-0.035 (-0.169, 0.099)	-0.013 (-0.125, 0.098)	26.1	20.5	0.184
Brachial, Radial, Tibial 35-55MHz	**LD**	56	2.500	2.485	0.004 (-0.146, 0.155)	-0.007 (-0.119, 0.105)	3.1	2.3	0.180
	IMT	57	0.18	0.183	0.003 (-0.036, 0.042)	-0.004 (-0.034, 0.026)	11.2	8.5	0.159
	IMAT	58	0.291	0.286	0.003 (-0.053, 0.058)	-0.000 (-0.045, 0.045)	9.8	8.1	0.265
	AT	58	0.11	0.103	-0.003 (-0.051, 0.045)	0.005 (-0.031, 0.041)	22.3	17.9	0.267

Table 3. *Inter-observer agreement of AMS and EC for different transducer frequencies, arterial sites and dimensions. LD – lumen dimension; IMT – intima-media thickness; IMAT – intima-media-adventitia thickness; AT – adventitia thickness; CV – coefficient of variation; ΔMean – mean difference; LOA 95% – 95% limits of agreement; AMS – semi-automatic border detection; EC – electronic calipers. From Sundholm et. al. 2014 (I), used with permission from Elsevier.*

Artery	Dimension	N	Mean thickness [mm] AMS	Mean thickness [mm] EC	ΔMean (LOA 95%) [mm] AMS	ΔMean (LOA 95%) [mm] EC	CV% AMS	CV% EC	p-value AMS vs EC
Carotid *25 MHz*	**LD**	20	5.555	5.503	0.082 (-0.864, 0.700)	0.112 (-0.516. 0.740)	7.2	5.8	0.191
	IMT	20	0.376	0.404	-0.008 (-0.108, 0.092)	-0.092 (-0.196. 0.013)	13.6	13.3	0.819
Femoral *25 MHz*	**LD**	20	7.623	7.665	-0.255 (-1.588, 1.077)	0.367 (-0.724. 1.458)	8.9	7.3	0.020
	IMT	20	0.325	0.327	0.001 (-0.113, 0.116)	0.005 (-0.117. 0.128)	18.0	19.1	0.905
	IMAT	20	0.576	0.618	-0.023 (-0.212, 0.165)	-0.034 (-0.292. 0.225)	16.7	21.4	0.045
	AT	20	0.251	0.291	-0.025 (-0.140, 0.091)	-0.039 (-0.252. 0.174)	23.4	37.4	0.050
Brachial, Radial, Tibial 35-55MHz	**LD**	60	2.474	2.455	-0.040 (-0.536, 0.455)	0.048 (-0.378. 0.475)	10.2	8.9	0.101
	IMT	60	0.183	0.183	0.002 (-0.055, 0.060)	-0.009 (-0.052. 0.035)	16.0	12.0	0.915
	IMAT	59	0.293	0.292	0.000 (-0.088, 0.088)	-0.015 (-0.095. 0.065)	15.3	9.8	0.290
	AT	60	0.110	0.109	-0.002 (-0.068, 0.063)	-0.007 (-0.078. 0.064)	30.3	33.3	0.644

Table 4. *Test-retest agreement of AMS and EC for different transducer frequencies, arterial sites and dimensions. LD – lumen dimension; IMT – intima-media thickness; IMAT – intima-media-adventitia thickness; AT – adventitia thickness; CV – coefficient of variation; ΔMean – mean difference; LOA 95% – 95% limits of agreement; AMS – semi-automatic border detection; EC – electronic calipers. From Sundholm et. al. 2014 (I), used with permission from Elsevier.*

4.2 STUDY II, FEASIBILITY, ACCURACY AND PRECISION OF VHRU IN NEONATES

The more superficial location of arteries in neonates, compared to adults, allows the use of higher frequencies for vascular imaging in the near field. We found that the carotid and femoral artery far wall was visible using a 35MHz transducer in all subjects, and the brachial artery visible in all using a 55MHz transducer. The femoral artery was visible using a 55MHz transducer in all neonates with a body weight less than 2200g, in some with a body weight of 2200-3600g and in none with a body weight above 3600g. Vascular wall dimensions were below the resolution of the 55MHz transducer in 20/50 brachial arteries and 14/50 femoral arteries. The abdominal aorta (depth 40-65mm) was unreachable with VHRU transducers (maximum penetrance 23mm) in all subjects.

Results for intra-observer, inter-observer, and test-retest agreements are presented in Tables 5-7, with no bias and good agreement for all measured arterial dimension. There were only minute differences between inter-observer and test-retest agreements compared to intra-tester agreements. This suggested very limited operator dependency and technical variance overall influencing reproducibility of the measurements.(202) The technical variability was higher for smaller dimensions with measurements performed at a level bordering the axial resolution limit of the transducer. Overall, these results were similar to the results of study I.

In a head-to-head comparison between CIMT measurements obtained using conventional HRU 12MHz and VHRU 35MHz transducers, the conventional 12MHz transducer was shown to grossly overestimate CIMT measurements among neonates. Our results for CIMT using VHRU (mean 0.17mm) were significantly lower than previously reported HRU-derived values (range 0.23-0.37 mm) and beyond the calculated axial resolution limit of > 0.25 mm for conventional HRU frequencies.(203-206) We did not find any histological data on CIMT in this age group, but histologically measured IMT in infants has been reported as 0.40-0.50mm in the aorta and 0.05-0.15mm in the coronary arteries.(21,24,39,207,208)

The results show that the axial resolution of conventional HRU frequencies is insufficient to measure CIMT in infants. VHRU, however, allow the non-invasive measurement of vascular wall layer dimensions of the carotid artery and proximal muscular arteries in neonates, whilst more distal arteries are too small precluding assessment with VHRU. The wall of the aorta is too deeply located to be visualized using VHRU, but the aortic IMT can be measured with the higher frequencies of the HRU-spectrum (10-20MHz) as previously reported.

The main limitations of the study were the small sample size and lack of histological verification of vascular dimensions. We did however include neonates of different gestational ages and body-sizes and assessed multiple arteries using different transducer frequencies allowing us to assess the feasibility of VHRU in the neonatal age group over all.

Artery	Dimension	N	Mean [mm]	ΔMean (LOA 95%) [mm]	CV%
CCA (35 MHz)	LD	38	2.619	0.000 (−0.107,0.107)	2.1
	IMT	40	0.158	−0.016 (−0.066, 0.035)	16.1
BA (55 MHz)	LD	40	1.445	−0.003 (−0.058, 0.052)	1.9
	IMT	24	0.062	−0.004 (−0.034, 0.026)	24.8
	IMAT	39	0.141	−0.013 (−0.064, 0.038)	18.5
	AT	25	0.085	−0.004 (−0.038, 0.031)	20.5
FA (35–55 MHz)	LD	37	1.794	−0.002 (−0.056, 0.053)	1.5
	IMT	37	0.068	−0.003 (−0.021, 0.014)	13.1
	IMAT	40	0.161	−0.013 (−0.066, 0.040)	16.8
	AT	32	0.092	0.004 (−0.042, 0.050)	25.6

Table 5. *Intra-observer variation for different neonatal arterial dimensions obtained with VHRU. ΔMean - mean difference; LOA 95% - 95% limits of agreement; CV% - coefficient of variation; CCA – common carotid artery ; BA – brachial Artery; FA – femoral artery; LD - lumen diameter; IMT - intima-media thickness; IMAT - intima-media-adventitia thickness; AT - adventitia thickness. From Sundholm et.al. 2015 (II), used with permission from Elsevier.*

Artery	Dimension	N	Mean [mm]	ΔMean (LOA 95%) [mm]	CV%
CCA (35 MHz)	LD	38	2.556	0.065 (−0.053, 0.184)	2.4
	IMT	38	0.165	−0.012 (−0.054, 0.029)	12.8
BA (55 MHz)	LD	40	1.432	0.035 (−0.049, 0.118)	3.0
	IMT	24	0.062	−0.001 (−0.026, 0.025)	21.1
	IMAT	40	0.141	−0.000 (−0.039, 0.039)	14.3
	AT	25	0.087	0.003 (−0.028, 0.034)	18.1
FA (35–55 MHz)	LD	39	1.772	0.045 (−0.052, 0.142)	2.8
	IMT	36	0.066	−0.002 (−0.022, 0.017)	15.4
	IMAT	38	0.160	0.002 (−0.025, 0.029)	8.8
	AT	31	0.091	−0.002 (−0.040, 0.036)	21.2

Table 6. *Inter-observer variation for different neonatal arterial dimensions obtained with VHRU. ΔMean - mean difference; LOA 95% - 95% limits of agreement; CV% - coefficient of variation; CCA, common carotid artery; BA - brachial artery; FA - femoral artery; LD - lumen diameter; IMT - intima-media thickness; IMAT - intima-media-adventitia thickness; AT - adventitia thickness. From Sundholm et.al. 2015 (II), used with permission from Elsevier.*

Artery	Dimension	N	Mean [mm]	ΔMean (LOA 95%) [mm]	CV%
CCA (35 MHz)	LD	10	2.671	0.103 (−0.352, 0.146)	4.8
	IMT	10	0.146	0.003 (−0.030, 0.036)	11.7
BA (55 MHz)	LD	10	1.417	0.076 (−0.145, 0.297)	8.0
	IMT	5	0.056	−0.004 (−0.022, 0.014)	16.0
	IMAT	10	0.113	−0.004 (−0.036, 0.028)	14.6
	AT	5	0.072	0.000 (−0.046, 0.046)	32.6
FA (35–55 MHz)	LD	10	1.769	0.002 (−0.190, 0.194)	5.6
	IMT	6	0.058	−0.002 (−0.09, 0.006)	7.1
	IMAT	10	0.144	0.003 (−0.028, 0.034)	10.9
	AT	6	0.087	−0.007 (−0.022, 0.036)	17.4

Table 7. *Test-retest variation for different neonatal arterial dimensions obtained with VHRU. ΔMean - mean difference; LOA 95% - 95% limits of agreement; CV% - coefficient of variation; CCA; BA – brachial artery; FA - femoral artery; LD - lumen diameter; IMT - intima-media thickness; IMAT - intima-media-adventitia thickness; AT - adventitia thickness. From Sundholm et.al. 2015 (II), used with permission from Elsevier.*

4.3 VALIDATION OF ULTRASOUND ARTERIAL INTIMA THICKNESS MEASUREMENT

Validation of VHRU IT and the four-line pattern

The distinct four-line pattern in muscular artery VHRU was consistent with intimal thickening in histology (Figure 13a and b). A separation of the first echogenic zone (Z1-Z3) allowed the leading-to-leading edge measurement of the intima thickness.

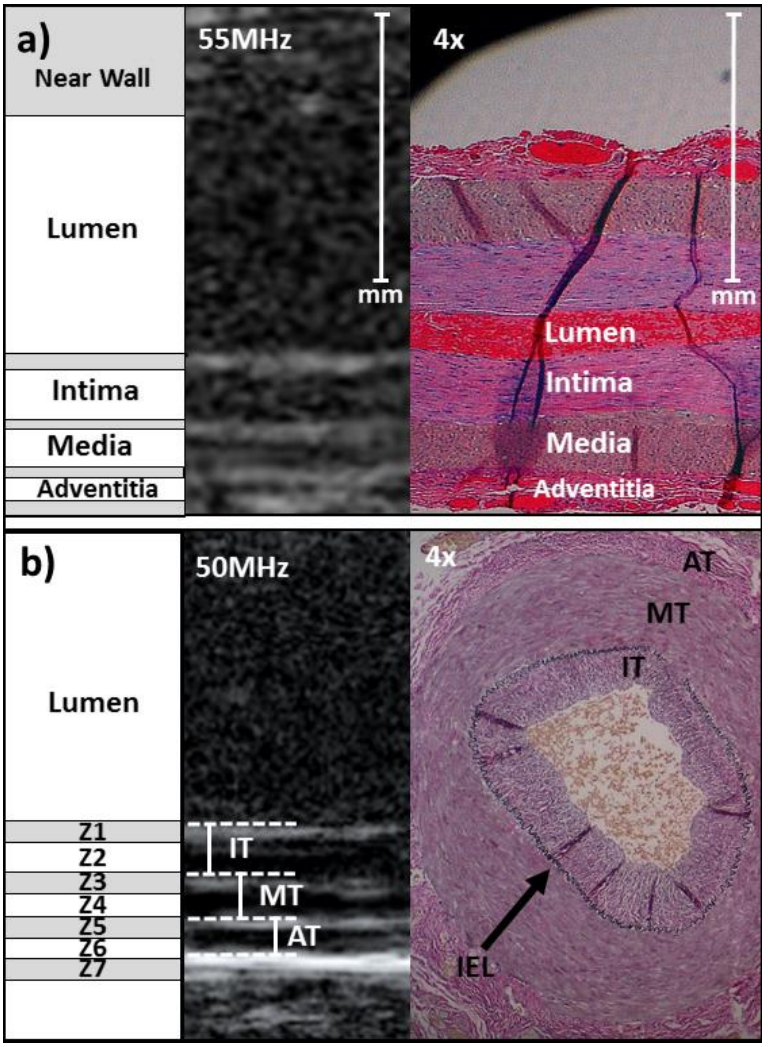

Figure 13. *Schematic, 55MHz VHRU-derived image, and corresponding histology of temporal arteries with evident intimal thickening. Leading edge borders are shown. IT – Intima; MT – Media; AT – Adventitia; IEL – Internal elastic laminae. Modified from Sundholm et.al. 2019 (III).*

Arterial layer thickness measurements of the first region (Z1-Z3) agreed well with histological IT and showed good intra- and inter-observer agreements. (Table 8-10). The four-line pattern was detected in 28/29 patients with histological IT>0.06mm and in none with thinner intima (sensitivity of 96.3%, CI95%: 81.0-99.9% and a specificity of 100%, CI95%: 66.3-100%). We did not find any significant difference in accuracy between the two ultrasound systems used (Vevo770 vs. VevoMD, ICC 0.867, CI95% 0.603-0.955 and 0.971 CI95% 0.901-0.992, respectively), with a trend for reduced accuracy for images of lower quality (CV% 12.8 vs. 23.6 p=0.098).

		Histology		**VHRU**				
		Mean	***SD***	***Mean***	***SD***	***ΔMean***		
	N	***[mm]***	***[mm]***	***[mm]***	***[mm]***	***[mm]***	***LOA 95%***	***CV%***
IT	28	0.125	0.045	0.132	0.050	0.007	-0.042;0.057	19.7
IMT	37	0.255	0.097	0.243	0.086	-0.012	-0.086;0.064	15.1

Table 8. *Comparison of histology and VHRU measurements of intima and intima-media thickness. SD -standard deviation; LOA – 95% limits of agreement; CV% - coefficient of variation (%); CI95% – 95% confidence interval; ΔMean – mean difference; IT – Intima thickness; IMT – Intima-media thickness. From Sundholm et.al. 2019 (III), used with permission from Elsevier.*

Intra-observer	**N**	**Mean [mm]**	**SD [mm]**	**ΔMean [mm]**	**LOA 95%**	**CV%**
IT	25	0.140	0.047	-0.011	-0.053; 0.032	15.7
IMT	31	0.246	0.090	-0.006	-0.085; 0.071	16.1

Table 9. *Intra--observer agreements for VHRU-derived intima and intima-media thicknesses. SD – standard deviation; LOA95% - 95% limits of agreement; CV% - Coefficient of variation (%); CI95% – 95% confidence interval; IT- Intima thickness; IMT – Intima-media thickness. From Sundholm et.al. 2019 (III), used with permission from Elsevier.*

Inter-observer	N	Mean [mm]	SD [mm]	ΔMean [mm]	LOA 95%	CV%
IT	25	0.136	0.044	0.012	-0.040;0.065	19.9
IMT	31	0.240	0.085	0.025	-0.075;0.125	21.2

Table 10. *Inter-observer agreements for VHRU-derived intima and intima-media thicknesses. SD – standard deviation; LOA95% - 95% limits of agreement; CV% - Coefficient of variation (%); CI95% – 95% confidence interval; IT- Intima thickness; IMT – Intima-media thickness. From Sundholm et.al. 2019 (III), used with permission from Elsevier.*

Measurements leading-to-trailing edge of the first echogenic zone (Z1-Z3) in subjects without a visible four-line pattern was not associated with histological IT (Figures 14 and 15). This is in line with previous validation attempts in arteries with healthy thin IT.(18,89) Leading-to-trailing edge measurements of IT in arteries with thickened IT, however, correlates well with histological IT, but systematically overestimates the dimension, an issue not seen with the leading-to-leading edge method.(69)

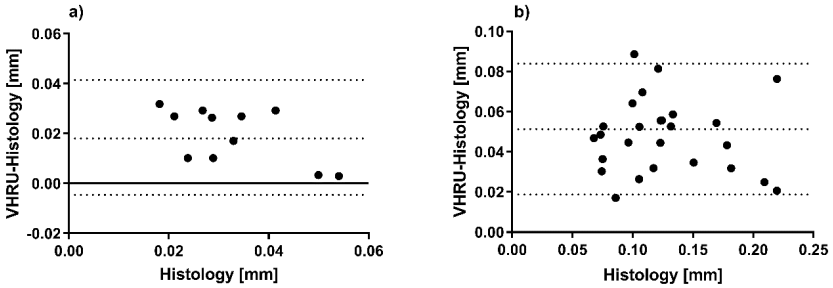

Figure 14. *Bland-Altmant plots comparing very-high resolution ultrasound (VHRU) intima layer thickness (IT) with histology IT using the leading-to-trailing edge measurement technique in the assessment of the VHRU image. a) Leading-to-trailing edge VHRU measurement of blood-intima interface (fused zones 1-3) in arteries with histological IT less than 0.06 mm. b) Leading-to-trailing edge VHRU measurement of the visible IT (zones 1-3 separated in image, measurement from leading-edge of zone 1 to trailing edge of zone 3) in arteries with histological IT 0.06 mm or more. Note the systematic bias in leading-to-trailing edge VHRU IT measurement in comparison to histological IT in both settings. From the supplemental material of Sundholm et.al. 2019 (III), used with permission from Elsevier.*

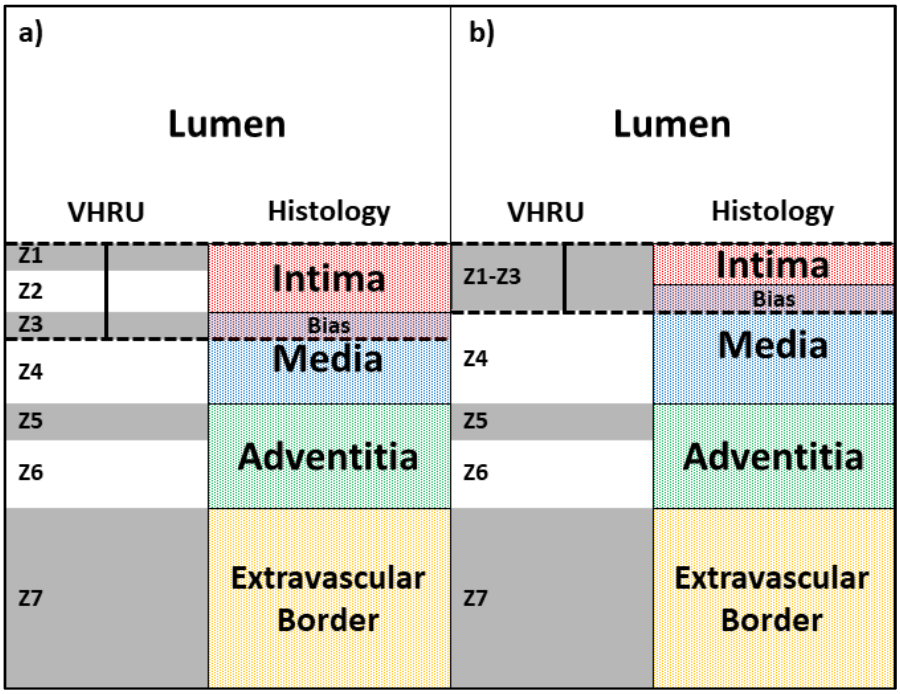

Figure 15*. Schematic image of how measures using the leading-to-trailing edge method induces bias in a) vessels with a thickened intima (separated zones 1-3). and b) vessels with a thin intima (fused zones 1-3). Note how the bias is equal to Z3 in case a). whereas the bias is influenced by the histological intima artery layer thickness (IT) in b) as Z1-Z3 remains constant and non-related with histological IT variance. From the supplemental material of Sundholm et.al. 2019 (III) used with permission from Elsevier.*

We conclude that VHRU-derived measurements of intima-thickness is accurate and reliable in arteries with an intimal thickness of >0.06mm corresponding to 5px with the 55MHz transducer. We further showed that the four-line pattern is increasing with age with 76% of the subjects aged 40 to 86 years showing a four-line pattern in the temporal artery and 68% in the radial artery in vivo using the highest 50-55 MHz ultrasound frequency. The four-line pattern was not visible in most carotid and brachial arteries, likely related to the lower 30-35 MHz ultrasound frequencies used for these anatomical locations for imaging depth reasons. We further preliminarily show that arterial IT in our sample is related to cardiovascular risk factors (Table 11).

These results suggest that the VHRU-derived vascular IT could be used to monitor vascular health and potentially as a non-invasive surrogate marker of cardiovascular disease in the aging population.

Dependent variable	**Adjusted R2**	**Model p-value**
Intima thickness [µm]	0.404	<0.001
Independent variables	**Beta**	**p-value**
Constant	-36.6	0.464
Age [years]	1.7	0.038
Hypertension [yes=1 no=0]	42.2	0.020
Diabetes [yes=1 no=0]	34.2	0.044
Hypercholesterolemia [yes=1 no=0]	-26.7	0.141
Smoking [10 pack years]	6.8	0.069

Table 11. *Linear regression model assessing effects of age and cardiovascular risk factors on histological intima thickness in the GCA sample (n=37). From the supplemental material of Sundholm et.al. 2019 (III), used with permission from Elsevier.*

The study was limited by histological verification of temporal arteries only. The study setting did, however, allow the direct comparison of *in vivo* VHRU measurements with histology in subjects with a wide range of vascular aging, spanning from a thin intima below axial resolution to pathological intimal thickening bordering early plaque formation. We further assessed vascular morphology using VHRU in multiple arteries and verified the presence of the four-line pattern in radial arteries to a similar extent as in temporal arteries.

4.4 DIAGNOSTIC UTILITY OF VHRU IN GIANT-CELL ARTERITIS

VHRU-derived intima thickness measurements and HRU-derived Halo-Doppler ratio (HDR) in the transmural inflammation GCA group differed significantly from GCA negative subjects and from clinical GCA patients with no or limited inflammation on histology, and without histological arterial wall layer thickening. (Table 12)

Specificity and sensitivity charts provided optimal diagnostic cut-off values for TMI >0.30mm for IT and 2.0 for HDR, yielding sensitivity 90.9%, CI95% 58.7-99.8%; specificity 100%, CI95% 91.1-100.0%; LHR+ N/A; LHR- 0.1 for IT and sensitivity 55.6%, CI95% 21.2-86.3%; specificity 93.5%, CI95% 77.9-99.1%; LHR+ 8.6, LHR- 0.5 for HDR, compared to the non-GCA group.

To assess diagnostic utility, the coded images were analysed by a second expert observer blinded to patient characteristics and biopsy results. Inter-observer agreements for diagnostic cut-off values were high (Cohen's Kappa: 0.873 for IT>0.3mm and 0.811 for HDR>2.0). ROC analysis showed good diagnostic utility for both IT measurements and HDR (AUC: VHRU-IT 0.99, CI95% 0.97-1.00; HRU-HDR 0.75, CI95% 0.54-0.96, p=0.026), with VHRU-derived IT outperforming HDR.

The diagnostic utility of HDR was found to be limited in subjects who had received glucocorticoid treatment for more than 5 days (Figure 16a). This is in line with previously published data.(164) In contrast, VHRU derived IT did not seem to be impacted by glucocorticoid treatment response to the same extent, and IT remained thickened for up to 37 day after treatment initiation (Figure 16b). The vascular wall of subjects with shorter duration of glucocorticoid treatment was fairly echolucent, making dimension borders challenging to distinguish (Figure 17). The results suggest that VHRU could be beneficial in GCA patient follow-up during glucocorticoid treatment in the outpatient setting.

Study group	Non-GCA N = 40	GCA, Biopsy negative N = 15	GCA, Inflammation limited to adventitia (ILA) N = 9	GCA, transmural inflammation (TMI) N = 11	p-value
HRU; N	31	9	7	9	
Halo	5 (16%)	1 (11%)	2 (29%)	5 (56%)	0.083
HDR	1.4 (1.0-2.8)	1.4 (1.2-1.9)	1.4 (1.0-4.2)	2.4 (1.5-9.3) [a]	0.007
HDR > 2.0	2 (6%)	0 (0%)	2 (29%)	5 (56%)[a]	0.003
VHRU; N	40	15	9	11	
Measurable IT; N	31	9	9	11	
Mean IT [mm]	0.12 (0.06-0.23)	0.09 (0.06-0.14)	0.14 (0.06-0.22)	0.28 (0.06-0.53)	<0.001
Max IT [mm]	0.16 (0.06-0.28)	0.11 (0.08-0.28)	0.16 (0.08-0.25)	0.40 (0.06-0.70) [a]	<0.001
Max IT > 0.30mm	0 (0%)	0 (0%)	0 (0%)	10 (91%)[a]	<0.001
IMT; N	40	15	9	11	
IMT [mm]	0.22 (0.08-0.42)	0.22 (0.09-0.29)	0.23 (0.17-0.28)	0.55 (0.22-0.834) [a]	<0.001
Max IMT [mm]	0.27 (0.09-0.49)	0.26 (0.10-0.43)	0.28 (0.18-0.55)	0.69 (0.31-1.10)	<0.001
Histology; N	37	12	9	11	
IT [mm]	0.11 (0.01-0.24)	0.09 (0.02-0.18)	0.14 (0.08-0.19)	0.38 (0.04-0.90) [a]	<0.001
MT [mm]	0.16 (0.05-0.36)	0.16 (0.08-0.25)	0.17 (0.11-0.34)	0.20 (0.11-0.41)	0.442
IMT [mm]	0.28 (0.07-0.49)	0.24 (0.10-0.41)	0.27 (0.24-0.50)	0.62 (0.15-1.31) [a]	<0.001
AT [mm]	0.06 (0.02-0.12)	0.06 (0.03-0.08)	0.07 (0.05-0.14)	0.14 (0.05-0.23) [a]	<0.001

Table 12. *Halo-Doppler ratio and vascular dimensions obtained with VHRU and histology. Results are presented as median (range) or N (%). P-values represent results for group comparisons with the Fisher-Freeman-Halton exact test (post-hoc: independent Fisher exact test with Bonferroni adjusted significance levels) and the Kruskal-Wallis tests (post-hoc: Dunn-Bonferroni). Note that IT was not measurable in VHRU imaged in subjects with IT<0.06mm.* [a] *– differs significantly from all other groups in post-hoc analysis at level p<0.05; IT – intima thickness; MT – media thickness; IMT – intima-media thickness; AT – adventitia thickness; VHRU – very-high resolution ultrasound; HRU – high resolution ultrasound; HDR – Halo-Doppler Ratio. From Sundholm et al. 2019 (IV).*

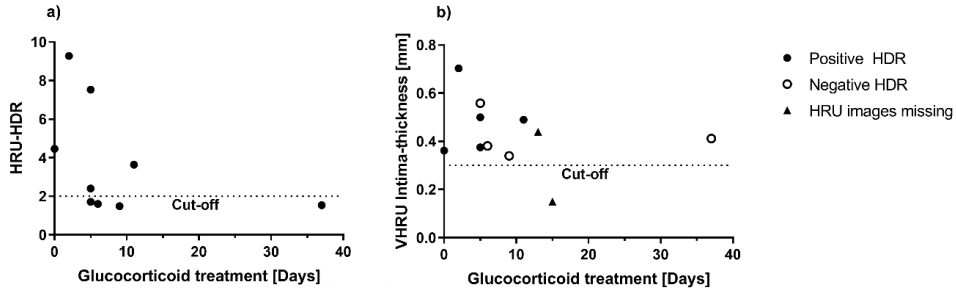

Figure 16 *a) Conventional ultrasound derived Halo-Doppler ratio versus glucocorticoid-treatment duration prior to imaging in the transmural inflammation (TMI) group. b) VHRU intima thickness versus glucocorticoid-treatment duration prior to imaging in TMI group. Note that the intimal thickness exceeds the diagnostic cut-off 0.3mm from 5 days of corticosteroid treatment, whereas the prevalence of the halo-sign cut-off >2.0 diminishes. HDR – Halo-Doppler ratio; HRU – Highresolution ultrasound; VHRU – Very-high resolution ultrasound. Modified from Sundholm et.al. 2019 (IV).*

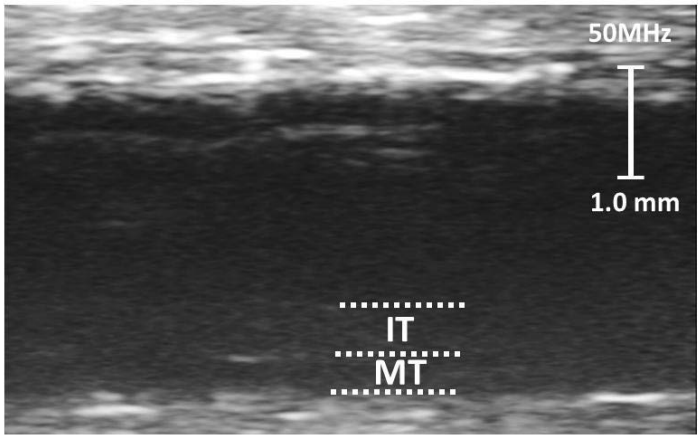

Figure 17. *Very-high resolution ultrasound image (50MHz) of a temporal artery with transmural inflammation after only 2 days of glucocorticoid treatment. Note the thick and dark vascular wall making the layer borders challenging to distinguish. IT – intima thickness; MT – media thickness. Modified from Sundholm et.al. 2019 (IV).*

Neither HDR or VHRU-IT showed any diagnostic utility in groups with limited or no inflammation on histology and a thin histological IT. This is in line with previous findings showing decreased diagnostic utility of the halo sign in this patient group.(153) The increased resolution of VHRU did not add further diagnostic value to these subjects.

The main limitation of this study is the evident delay in ultrasound assessment, with imaging performed, in many cases, following several days of glucocorticoid treatment. This most likely affected the diagnostic utility of the halo-sign, reducing comparability with previous studies, but allowed a direct comparison of VHRU images and histology.

5. CONCLUSIONS

I. The use of a semi-automatic border detection software is, feasible, accurate and precise for very-high resolution ultrasound image analysis of arterial intima-media thickness and adventitia thickness, with reduced analysis time compared to electronic calipers.

II. The arterial wall layer thickness in infants is below the axial resolution, and thus unmeasurable, using conventional high-resolution ultrasound frequencies. The increased resolution of very-high resolution ultrasound allows accurate and precise non-invasive measurements of the carotid intima-media thickness, in addition to brachial and femoral arterial intima-media thickness and adventitia thickness in neonates *in vivo.*

III. The identification of a distinct four-line pattern with very-high resolution ultrasound imaging of the arterial far wall allows the non-invasive quantification of intima layer thickness in superficial arteries of the aging population. The finding is consistent with changes in the intima occurring with arterial aging.

IV. Very-high resolution ultrasound derived measurements of temporal artery intima layer thickness allows the non-invasive real time diagnosis of transmural inflammation related intimal thickening of the temporal artery in patient with suspected giant cell arteritis. The very-high resolution ultrasound detected vascular wall thickening was evident in most patients with transmural inflammation, and this diagnostic marker is more sensitive than the conventional high-resolution ultrasound derived Halo-Doppler-ratio in patients with prolonged glucocorticoid treatment. Neither the VHRU-method nor the Halo-Doppler ratio showed diagnostic utility in patients with no inflammation or inflammation limited to the adventitia on histology.

6. PERSPECTIVES AND FUTURE RESEARCH TOPICS

This thesis presents very-high resolution ultrasound as a tool to investigate vascular morphology and pathology *in vivo.* We show that the increased resolution allows for assessment of vascular structure in almost microscopical detail. This provides the opportunity for a new field of different research topics.

Most previous studies assessing distal vascular morphology in different age groups are based on post-mortem data, and thus limited sample sizes. This emerging method allows for investigation and follow-up of larger populations. It is now possible to non-invasively assess factors related with vascular morphology, pathology, and changes in vascular structures with aging. This is an interesting new field of research that could give us further knowledge on vascular health and diseases.

Carotid intima-media thickness has been used as a surrogate marker for cardiovascular risk for three decades. The method isn't flawless, and the utility is limited in a clinical setting.(7) The increased resolution of very-high resolution ultrasound provides more detailed information of the vascular wall than the established high-resolution ultrasound method, and the increased resolution could also improve measurement accuracy and reduce absolute measurement errors. Future research topics could address not only peripheral conduit artery intima-media thickness, but also intima thickness in relation to cardiovascular risk.

The non-invasive nature and versatility of conventional ultrasound has established its role as a diagnostic tool in peripheral artery disease.(209) The method is, however, limited when studying the smallest arteries due to limited resolution. Further research could assess the utility of VHRU when assessing severity of peripheral artery disease.

Our results indicate that, compared with HRU, VHRU used as a diagnostic tool to assess suspected giant cell arteritis of the temporal artery could be more sensitive for patients with several days of ongoing glucocorticoid treatment. Current guidelines state that imaging should be performed prior to or during the first days of

treatment.(172) Further studies should compare VHRU and HRU methods in a pretreatment setting. Another interesting topic would be to assess the utility of VHRU as method to non-invasively and prospectively monitor changes in the vascular wall in response to treatment.

7. YHTEENVETO (FINNISH SUMMARY)

Kajoamaton korkeataajuusultraääni (VHRU, very-high resolution ultrasound, 25-55MHz) on 2000-luvulla kehitetty ultraäänimenetelmä valtimonseinämän kuvantamiseen. Korkeammilla ultraäänitaajuuksilla kuvan erottelukyky on parempi, lähes mikroskooppitasoa, mutta kuvausalue on rajoittunut lähellä anturia oleviin rakenteisiin. Menetelmä soveltuu erinomaisesti aikuisten pinnallisten valtimoiden ja lasten pienten valtimoiden valtimoseinämän kajoamattomaan kuvantamiseen. Tässä väitöskirjassa arvioidaan puoliautomaattisen analyysiohjelman käyttöä valtimoseinämän eri kerrosten mittaamisessa. Lisäksi kirjassa selvitetään menetelmän soveltuvuutta vastasyntyneiden lasten valtimoseinämän arvioinnissa, menetelmän käyttöä valtimon sisäkalvon (*tunica intima*) paksuuden mittauksessa ikääntyneillä, sekä menetelmän hyötyjä jättisoluarteriitin diagnostiikassa.

Tutkimme puoliautomaattisen ohjelman (AMS, *arterial measurement systems*) käyttöä kymmenen henkilön eri verisuonista otettujen kuvien arvioinnissa vertailemalla analyysiaikaa ja mittauksien luotettavuutta käsin tehtyihin yksittäismittauksiin. Emme löytäneet eroa menetelmien luotettavuudessa, mutta puoliautomaattisen menetelmän analyysiaika oli merkittävästi lyhyempi. Mittausten suhteellinen tekninen vaihtelu liittyi lähinnä kuvanlaatuun ja mitattavaan etäisyyteen.

Vertasimme kymmenestä vastasyntyneestä VHRU-menetelmällä ja tavallisella ultraäänellä otettuja kuvia. VHRU-menetelmä pystyi luotettavasti ja tarkasti mittaamaan suurten ja keskisuurten valtimoiden seinämän kerrospaksuudet, mutta tavallisen ultraäänen erottelukyky ei ollut riittävä. VHRU-menetelmän erottelukyky ei ollut riittävä pienempien ääreisvaltimoiden, esimerkiksi värttinävaltimon, seinämän kerrosten arvioinnissa.

VHRU-menetelmällä tutkittiin 78 ikääntynyttä potilasta, jotka oli lähetetty ohimovaltimon koepalan ottoon jättisoluarteriittiepäilyn takia. Niiden potilaiden joukossa, joilla ei ollut tulehdusmuutoksia suonen seinämässä (biopsia-negatiiviset), 76 %:lla oli histologisesti paksuuntunut valtimon sisäkalvo (*tunica intima*), joka oli

tarkasti ja luotettavasti mitattavissa VHRU-menetelmällä. Jättisoluarteriittipotilailla ohimovaltimon seinämä oli histologiassa selkeästi paksuntunut. VHRU-menetelmällä mitattu yli 0.3 mm:n valtimon sisäkalvo oli tarkka ja herkkä mittari jättisoluarteriitille, ja se oli todettavissa 10/11 potilaalla.

Kajoamaton korkeataajuusultraääni on uusi menetelmä, jolla pinnallisten valtimoiden seinämän kerrosten paksuudet voidaan tarkasti ja luotettavasti mitata. Puoliautomaattisella ohjelmalla valtimoseinämän kerroksen paksuuden mittaamista voidaan nopeuttaa. Menetelmän parempi erottelukyky mahdollistaa pienten vastasyntyneiden valtimoseinämän kuvantamisen ja ikääntyvien valtimon sisäkalvon (*tunica intima*) paksuuden mittaamisen. Ohimovaltimon jättisoluarteriitissa suonenseinämä turpoaa tulehduksen seurauksena ja tämä näkyy VHRU-kuvissa paksuuntuneena sisäkalvona (*tunica intima*). Menetelmä voisi tulevaisuudessa soveltua kliiniseen käyttöön pinnallisten verisuonisairauksien tutkimuksessa ja diagnostiikassa.

8. SAMMANFATTNING (SWEDISH SUMMARY)

Icke-invasivt högresolutionsultraljud (VHRU, *very-high resolution ultrasound)* är en ny under 2000-talet utvecklad metod för undersökning av kärlväggen. Den höga ultraljudsfrekvensen ger en bättre, nästan mikroskopisk, resolution i ultraljudsbilden, men den lämpar sig endast för avbildning av närliggande strukturer. Med metoden kan den ytliga artärväggens olika skikt och små barns artärer avbildas. I den här avhandlingen utreder vi möjligheten att i ultraljudsbilden mäta artärväggens skikttjocklek med hjälp av en halvautomatisk metod. Vi utreder dessutom möjligheten att undersöka artärväggen hos nyfödda barn, att mäta artärväggens innersta lagrets (*tunica intima*) tjocklek hos den åldrande populationen, samt utreder nyttan av VHRU vid diagnostik av misstänkt jättecellsarterit.

Vi tillämpade ett halvautomatiskt analysprogram (AMS, *arterial measurement systems)* på VHRU-bilder tagna från ytliga artärer från tio personer och jämförde analystiden samt pålitligheten (precisionen) av de halvautomatiska mätningarna med enskilda manuella mätningar. Pålitligheten var jämförbar men analystiden var signifikant kortare. Pålitligheten var främst relaterad till bildkvaliteten och det uppmätta avståndet.

Vi jämförde bilder av ytliga muskulära artärer hos tio nyfödda barn och prematurer tagna med både VHRU-metoden och konventionellt ultraljud. VHRU-metoden kunde noggrant och pålitligt mäta artväggens skikttjocklek i stora och medelstora artärer medan det konventionella ultraljudets resolution var otillräckligt. VHRU-metodens resolution var otillräcklig för bedömning av artärväggens skikttjocklek i mindre och mera perifera kärl så som i strålbensartären.

Vi undersökte tinningartären med VHRU-metoden hos 78 äldre patienter remitterade för biopsi av tinningartären på grund av misstänkt jättecellsarterit. Bland patienter utan histologiskt påvisbar inflammation i artärväggen (negativ biopsi) konstaterades ett åldersrelaterat förtjockat inre skikt (*tunica intima*) hos 76% som noggrant och pålitligt kunde mätas i ultraljudsbilden. Ett förtjockat inre skikt (*tunica*

intima), mer än 0,3 mm i ultraljudsbilden, var ett specifikt och sensitivt fynd för jättecellsarteriten, och kunde konstateras hos 10/11 patienter.

Sammanfattningsvis är högresolutionsultraljud en ny metod för icke-invasiv undersökning av ytliga artärers kärlvägg. Tillämpningen av ett halvautomatiskt program i bildanalysen var pålitligt och försnabbade analysprocessen. Metodens höga resolution möjliggör avbildning av den ytliga artväggen hos nyfödda samt en mätning av ett förtjockat inre skikt (*tunica intima*) i artärväggen i den åldrande populationen. Jättecellsarterit av tinningartären ger upphov till en uppsvullen kärlvägg och det kraftigt förtjockade inre skiktet (*tunica intima*) kan icke-invasivt mätas med VHRU vid misstänkt jättecellsarterit. Metoden kan i framtiden få en viktig roll inom den kliniska diagnostiken av ytlig vaskulärpatologi och i studier av vaskulärt åldrande.

9. ACKNOWLEDGEMENTS

This study was carried out at the Children's Hospital, as well as at the GE-center at University of Helsinki and Helsinki University Hospital, Finland. I wish to acknowledge those who have provided me with research facilities: Docent *Jari Petäjä*, Director of the Children's Hospital; Docent *Eero Jokinen* Head of Tertiary Pediatrics; Docent *Esko Kemppainen* Director of the GE-center; Docent *Anders Albäck*; Head of Vascular Surgery; Professor *Klaus Olkkola*, Head of the Institute of Clinical Medicine; Professor *Markku Heikinheimo* the chairman of the Children's Hospital; and Professor *Pauli Puolakkainen* the chairman of the Department of Surgery.

I further wish to thank the Head of the Doctoral Programme at Children's Hospital Professor *Kim Vettenranta* and the Head of the Doctoral Programme in Clinical Research and Head of the Pediatric Research Center, Professor *Taneli Raivio* for providing me with valuable education supporting my research work.

This study was funded with support from numerous funds. I wish to thank Sigrid Jusélius Foundation, The Medical Society of Finland, and Finnish Foundation for Pediatric Research, Perklén foundation, Medicinska understödsföreningen Liv och Hälsa, and the Stockmann Foundation for financially supporting this study.

I want to acknowledge the official reviewers, Docent *Heikki Valleala* and Professor *Juhani Knuuti* for their expertise and valuable comments on this thesis. I further want to thank my thesis committee Docent *Risto Lapatto* and Docent *Kirsi Lauerma* and Custos Professor *Markku Heikinheimo* for their support with this project.

I want to thank my supervisor *Taisto Sarkola* for allowing me to join his research group and introducing me to the scientific method. It was in 2011, when I as a medical student first met Taisto who was to become my supervisor. Little did I know that it would become a 8-year collaboration, which would result in this thesis. I'm truly grateful for everything you have thought me, the sense of quality, the attention for detail, the importance of rigid scientific methods, and art of scientific writing. I could not have asked for a better supervisor for my project. Your expertise, your active tuition and swift communication made the project possible.

This thesis allowed me to work with numerous outstanding co-authors. I'm truly grateful to have had the opportunity to work with Professor *Tom Pettersson,* Docent *Anders Albäck,* Docent *Anders Paetau,* and I'm thankful for their help with planning and fulfilling my project. Your contributions have been immensely valuable for the project and I had your support throughout. I want to thank my fellow PhD-student Doctor *Rasmus Olander* for the peer support and collaboration throughout the years. I further wish to thank co-authors Professor *Sture Andersson*, Professor *Tomas Gustavsson*, and Docent *Tiina Ojala* for their valuable contributions to this project and Nurse Manager *Helena Raappana* and the staff at the Vascular Surgery unit for aid with recruitment.

I further wish to thank my family and friends for all their support, my dear parents *Maj-Len* and *Dage Sundholm* for all the support throughout my studies. I'm most grateful for you being there whenever I've needed, helped me through difficult times, you've shown interest in my work, and, perhaps without you knowing, through our discussions spurred my inspiration to research further, finding new topics. I don't think it's a coincidence that I've ended up doing what I do. My father introduced me to the world of science at an (too?) early age, giving me a scientific hunger that has been following me all my life. My mother always thought me to remember the humane side of life, that empathy is as important, or even more, than scientific advance. I wish to thank my brother *Mathias* for our life-long friendship. You have assisted me with your technological expertise, challenging me to step out of my comfort zone, and learn the technical limitations of my method, and how to overcome them.

I want to thank all my friends that have tolerated me for past years, and hopefully will for years to come. If all the hours spent discussing various topics in the sauna with *Kyrkslätts glada bastare,* or at lunch with *Flyga DoktorAnd -klubben* would've been spent on research I might have finished my thesis years ago, but it wouldn't have been nearly as fun.

I'll give my cat *Kex* a mention as well. I'm glad you didn't sit on my keyboard 100% of the time. Your contribution to my writing would have been far more helpful if your paws could write.

10. REFERENCES

(1) Pignoli P. Ultrasound B-mode imaging for arterial wall thickness measurement. Atherosclerosis Reviews 1984(12):177-184.

(2) Pignoli P, Tremoli E, Poli A, Oreste P, Paoletti R. Intimal plus medial thickness of the arterial wall: a direct measurement with ultrasound imaging. Circulation 1986(6):1399-1406.

(3) Wendelhag I, Gustavsson T, Suurkula M, Berglund G, Wikstrand J. Ultrasound measurement of wall thickness in the carotid artery: fundamental principles and description of a computerized analysing system. Clin Physiol 1991(6):565-577.

(4) Stein JH, Korcarz CE, Hurst RT, Lonn E, Kendall CB, Mohler ER, et al. Use of carotid ultrasound to identify subclinical vascular disease and evaluate cardiovascular disease risk: a consensus statement from the American Society of Echocardiography Carotid Intima-Media Thickness Task Force. Endorsed by the Society for Vascular Medicine. J Am Soc Echocardiogr 2008(2):93-111; quiz 189-90.

(5) Lorenz MW, Gao L, Ziegelbauer K, Norata GD, Empana JP, Schmidtmann I, et al. Predictive value for cardiovascular events of common carotid intima media thickness and its rate of change in individuals at high cardiovascular risk - Results from the PROG-IMT collaboration. PLoS One 2018(4):e0191172.

(6) Williams B, Mancia G, Spiering W, Agabiti Rosei E, Azizi M, Burnier M, et al. 2018 ESC/ESH Guidelines for the management of arterial hypertension. Eur Heart J 2018(33):3021-3104.

(7) Goff DC,Jr, Lloyd-Jones DM, Bennett G, Coady S, D'Agostino RB S, Gibbons R, et al. 2013 ACC/AHA guideline on the assessment of cardiovascular risk: a report of the American College of Cardiology/American Heart Association Task Force on Practice Guidelines. J Am Coll Cardiol 2014(25 Pt B):2935-2959.

(8) Sarkola T, Manlhiot C, Slorach C, Bradley TJ, Hui W, Mertens L, et al. Evolution of the arterial structure and function from infancy to adolescence is related to anthropometric and blood pressure changes. Arterioscler Thromb Vasc Biol 2012(10):2516-2524.

(9) McDicken WN, Anderson T. CHAPTER 1 - Basic physics of medical ultrasound. 2011:3-15.

(10) Szabo TL. Wave Scattering and Imaging. Diagnostic Ultrasound Imaging: Inside Out Oxford: Academic Press; 2014. p. 257-294.

(11) Abu-Zidan FM, Hefny AF, Corr P. Clinical ultrasound physics. J Emerg Trauma Shock 2011(4):501-503.

(12) Swanevelder J, Ng A. Resolution in ultrasound imaging. BJAed 2011(5):186-192.

(13) Jensen JA. Medical ultrasound imaging. Progress in Biophysics and Molecular Biology 2007(1):153-165.

(14) Lindner JR. Intimal Imaging With Ultrasound: What Anatomy Are We Resolving? Journal of the American Society of Echocardiography 2009(10):1134-1136.

(15) Hangiandreou NJ. AAPM/RSNA physics tutorial for residents. Topics in US: B-mode US: basic concepts and new technology. Radiographics 2003(4):1019-1033.

(16) Szabo TL. Attentuation. Diagnostic Ultrasound Imaging: Inside Out Oxford: Academic Press; 2014. p. 82-117.

(17) Foster FS, Pavlin CJ, Harasiewicz KA, Christopher DA, Turnbull DH. Advances in ultrasound biomicroscopy. Ultrasound Med Biol 2000(1):1-27.

(18) Sarkola T, Redington A, Keeley F, Bradley T, Jaeggi E. Transcutaneous very-high-resolution ultrasound to quantify arterial wall layers of muscular and elastic arteries: Validation of a method. Atherosclerosis 2010(2):516-523.

(19) Ross MH, Pawlina W. 13: Cardivascular System. Histology : a text and atlas : with correlated cell and molecular biology. Eight Edition ed.: Wolters Kluwer/Lippincott Williams & Wilkins Health; 2020. p. 432-471.

(20) Kölliker A. Of The Blood Vessels: Arteries. In: Busk G, Huxley T, editors. Manual of Human Histology. 2nd ed. London: The Sydenham Society; 1854. p. 294-301.

(21) Velican D, Velican C. Comparative study on age-related changes and atherosclerotic involvement of the coronary arteries of male and female subjects up to 40 years of age. Atherosclerosis 1981(1-2):39-50.

(22) Van Meurs Van Woezik H, Klein HW, Markus Silvis L, Krediet P. Comparison of the growth of the tunica media of the ascending aorta, aortic isthmus and descending aorta in infants and children. J Anat 1983(2):273-281.

(23) Witter K, Tonar Z, Schopper H. How many Layers has the Adventitia? - Structure of the Arterial Tunica Externa Revisited. Anat Histol Embryol 2017(2):110-120.

(24) Nakashima Y, Chen Y, Kinukawa N, Sueishi K. Distributions of diffuse intimal thickening in human arteries: preferential expression in atherosclerosis-prone arteries from an early age. Virchows Archiv 2002(3):279-288.

(25) Wilens SL. The Nature of Diffuse Intimal Thickening of Arteries. Am J Pathol 1951(5):825-839.

(26) Collins JA, Munoz JV, Patel TR, Loukas M, Tubbs RS. The anatomy of the aging aorta. Clin Anat 2014(3):463-466.

(27) Enos WF, Holmes RH, Beyer J. Coronary disease among United States soldiers killed in action in Korea; preliminary report. J Am Med Assoc 1953(12):1090-1093.

(28) McNamara JJ, Molot MA, Stremple JF, Cutting RT. Coronary artery disease in combat casualties in Vietnam. JAMA 1971(7):1185-1187.

(29) Mönckeberg J. Über die Atherosklerose der Kombattanten (nach Obduktionsbefunden). Zentralbl Herz Gefäßkrankheiten 1915(7):7-10.

(30) Virmani R, Avolio AP, Mergner WJ, Robinowitz M, Herderick EE, Cornhill JF, et al. Effect of aging on aortic morphology in populations with high and low prevalence of hypertension and atherosclerosis. Comparison between occidental and Chinese communities. Am J Pathol 1991(5):1119-1129.

(31) Spina M, Garbisa S, Hinnie J, Hunter JC, Serafini-Fracassini A. Age-related changes in composition and mechanical properties of the tunica media of the upper thoracic human aorta. Arteriosclerosis 1983(1):64-76.

(32) Hartman JD. Structural changes within the media of coronary arteries related to intimal thickening. Am J Pathol 1977(1):13-34.

(33) Mauriello A, Orlandi A, Palmieri G, Spagnoli LG, Oberholzer M, Christen H. Age-related modification of average volume and anisotropy of vascular smooth muscle cells. Pathol Res Pract 1992(4-5):630-636.

(34) Nilsson PM. Hemodynamic Aging as the Consequence of Structural Changes Associated with Early Vascular Aging (EVA). Aging Dis 2014(2):109-113.

(35) Sun Z. Aging, arterial stiffness, and hypertension. Hypertension 2015(2):252-256.

(36) Orlandi A, Mauriello A, Marino B, Spagnoli LG. Age-related modifications of aorta and coronaries in the rabbit: a morphological and morphometrical assessment. Arch Gerontol Geriatr 1993(1):37-53.

(37) Burton AC. Relation of structure to function of the tissues of the wall of blood vessels. Physiol Rev 1954(4):619-642.

(38) Friedman MH. A biologically plausible model of thickening of arterial intima under shear. Arteriosclerosis 1989(4):511-522.

(39) Movat HZ, More RH, Haust MD. The diffuse intimal thickening of the human aorta with aging. Am J Pathol 1958(6):1023-1031.

(40) Laina A, Stellos K, Stamatelopoulos K. Vascular ageing: Underlying mechanisms and clinical implications. Exp Gerontol 2018:16-30.

(41) Tesauro M, Mauriello A, Rovella V, Annicchiarico-Petruzzelli M, Cardillo C, Melino G, et al. Arterial ageing: from endothelial dysfunction to vascular calcification. J Intern Med 2017(5):471-482.

(42) Stary HC, Blankenhorn DH, Chandler AB, Glagov S, Insull W,Jr, Richardson M, et al. A definition of the intima of human arteries and of its atherosclerosis-prone regions. A report from the Committee on Vascular Lesions of the Council on Arteriosclerosis, American Heart Association. Circulation 1992(1):391-405.

(43) Nakashima Y, Wight TN, Sueishi K. Early atherosclerosis in humans: role of diffuse intimal thickening and extracellular matrix proteoglycans. Cardiovascres 2008(1):14-23.

(44) Kaprio J, Norio R, Pesonen E, Sarna S. Intimal thickening of the coronary arteries in infants in relation to family history of coronary artery disease. Circulation 1993(6):1960-1968.

(45) Abdelbaky A, Corsini E, Figueroa AL, Fontanez S, Subramanian S, Ferencik M, et al. Focal arterial inflammation precedes subsequent calcification in the same location: a longitudinal FDG-PET/CT study. Circ Cardiovasc Imaging 2013(5):747-754.

(46) Demer LL, Tintut Y. Inflammatory, metabolic, and genetic mechanisms of vascular calcification. Arterioscler Thromb Vasc Biol 2014(4):715-723.

(47) Kolodgie FD, Burke AP, Nakazawa G, Virmani R. Is pathologic intimal thickening the key to understanding early plaque progression in human atherosclerotic disease? Arterioscler Thromb Vasc Biol 2007(5):986-989.

(48) Virmani R, Kolodgie FD, Burke AP, Farb A, Schwartz SM. Lessons from sudden coronary death: a comprehensive morphological classification scheme for atherosclerotic lesions. Arterioscler Thromb Vasc Biol 2000(5):1262-1275.

(49) Xu X, Wang B, Ren C, Hu J, Greenberg DA, Chen T, et al. Age-related Impairment of Vascular Structure and Functions. Aging Dis 2017(5):590-610.

(50) Lockwood GR, Ryan LK, Hunt JW, Foster FS. Measurement of the ultrasonic properties of vascular tissues and blood from 35-65 MHz. Ultrasound Med Biol 1991(7):653-666.

(51) Gussenhoven EJ, Essed CE, Frietman P, van Egmond F, Lancee CT, van Kappellen WH, et al. Intravascular ultrasonic imaging: histologic and echographic correlation. Eur J Vasc Surg 1989(6):571-576.

(52) Persson J, Formgren J, Israelsson B, Berglund G. Ultrasound-determined intima-media thickness and atherosclerosis. Direct and indirect validation. Arterioscler Thromb 1994(2):261-264.

(53) Wong M, Edelstein J, Wollman J, Bond MG. Ultrasonic-pathological comparison of the human arterial wall. Verification of intima-media thickness. Arterioscler Thromb Vasc Bio 1993(4):482-486.

(54) Gamble G, Beaumont B, Smith H, Zorn J, Sanders G, Merrilees M, et al. B-mode ultrasound images of the carotid artery wall: correlation of ultrasound with histological measurements. Atherosclerosis 1993(2):163-173.

(55) Salonen R, Salonen JT. Determinants of carotid intima-media thickness: a population-based ultrasonography study in eastern Finnish men. J Intern Med 1991(3):225-231.

(56) George JM, Bhat R, Pai KM, S A, Jeganathan J. The carotid intima media thickness: a predictor of the clincal coronary events. J Clin Diagn Res 2013(6):1082-1085.

(57) Heiss G, Sharrett AR, Barnes R, Chambless LE, Szklo M, Alzola C. Carotid atherosclerosis measured by B-mode ultrasound in populations: associations with cardiovascular risk factors in the ARIC study. Am J Epidemiol 1991(3):250-256.

(58) Bots ML, Hoes AW, Koudstaal PJ, Hofman A, Grobbee DE. Common carotid intima-media thickness and risk of stroke and myocardial infarction: the Rotterdam Study. Circulation 1997(5):1432-1437.

(59) Chambless LE, Heiss G, Folsom AR, Rosamond W, Szklo M, Sharrett AR, et al. Association of coronary heart disease incidence with carotid arterial wall thickness and major risk factors: the Atherosclerosis Risk in Communities (ARIC) Study, 1987-1993. Am J Epidemiol 1997(6):483-494.

(60) O'Leary DH, Polak JF, Kronmal RA, Kittner SJ, Bond MG, Wolfson SK,Jr, et al. Distribution and correlates of sonographically detected carotid artery disease in the Cardiovascular Health Study. The CHS Collaborative Research Group. Stroke 1992(12):1752-1760.

(61) Rosvall M, Janzon L, Berglund G, Engstrom G, Hedblad B. Incident coronary events and case fatality in relation to common carotid intima-media thickness. J Intern Med 2005(5):430-437.

(62) Lorenz MW, Schaefer C, Steinmetz H, Sitzer M. Is carotid intima media thickness useful for individual prediction of cardiovascular risk? Ten-year results from the Carotid Atherosclerosis Progression Study (CAPS). Eur Heart J 2010(16):2041-2048.

(63) Lorenz MW, Markus HS, Bots ML, Rosvall M, Sitzer M. Prediction of clinical cardiovascular events with carotid intima-media thickness: a systematic review and meta-analysis. Circulation 2007(4):459-467.

(64) Den Ruijter HM, Peters SA, Anderson TJ, Britton AR, Dekker JM, Eijkemans MJ, et al. Common carotid intima-media thickness measurements in cardiovascular risk prediction: a meta-analysis. JAMA 2012(8):796-803.

(65) Naqvi TZ, Lee MS. Carotid intima-media thickness and plaque in cardiovascular risk assessment. JACC Cardiovasc Imaging 2014(10):1025-1038.

(66) Polak JF, Szklo M, O'Leary DH. Carotid Intima-Media Thickness Score, Positive Coronary Artery Calcium Score, and Incident Coronary Heart Disease: The Multi-Ethnic Study of Atherosclerosis. J Am Heart Assoc 2017(1):10.1161/JAHA.116.004612.

(67) Touboul PJ, Hennerici MG, Meairs S, Adams H, Amarenco P, Bornstein N, et al. Mannheim carotid intima-media thickness and plaque consensus (2004-2006-2011). An update on behalf of the advisory board of the 3rd, 4th and 5th watching the risk symposia, at the 13th, 15th and 20th European Stroke Conferences, Mannheim, Germany, 2004, Brussels, Belgium, 2006, and Hamburg, Germany, 2011. Cerebrovasc Dis 2012(4):290-296.

(68) Wikstrand J. Methodological considerations of ultrasound measurement of carotid artery intima-media thickness and lumen diameter. Clin Physiol Funct Imaging 2007(6):341-345.

(69) Osika W, Dangardt F, Gronros J, Lundstam U, Myredal A, Johansson M, et al. Increasing peripheral artery intima thickness from childhood to seniority. Arterioscler Thromb Vasc Biol 2007(3):671-676.

(70) Wikstrom J, Gronros J, Bergstrom G, Gan LM. Functional and morphologic imaging of coronary atherosclerosis in living mice using high-resolution color Doppler echocardiography and ultrasound biomicroscopy. J Am Coll Cardiol 2005(4):720-727.

(71) Gan LM, Gronros J, Hagg U, Wikstrom J, Theodoropoulos C, Friberg P, et al. Non-invasive real-time imaging of atherosclerosis in mice using ultrasound biomicroscopy. Atherosclerosis 2007(2):313-320.

(72) Eklund C, Friberg P, Gan LM. High-resolution radial artery intima-media thickness and cardiovascular risk factors in patients with suspected coronary artery disease--comparison with common carotid artery intima-media thickness. Atherosclerosis 2012(1):118-123.

(73) Eklund C, Omerovic E, Haraldsson I, Friberg P, Gan LM. Radial artery intima-media thickness predicts major cardiovascular events in patients with suspected coronary artery disease. Eur Heart J Cardiovasc Imaging 2014(7):769-775.

(74) Sarkola T, Jaeggi E, Slorach C, Hui W, Bradley T, Redington AN. Assessment of vascular remodeling after the Fontan procedure using a novel very high resolution ultrasound method: arterial wall thinning and venous thickening in late follow-up. Heart Vessels 2013(1):66-75.

(75) Olander RF, Sundholm JK, Ojala TH, Andersson S, Sarkola T. Neonatal Arterial Morphology Is Related to Body Size in Abnormal Human Fetal Growth. Circ Cardiovasc Imaging 2016(9):10.1161/CIRCIMAGING.116.004657.

(76) Sundholm JKM, Litwin L, Rönö K, Koivusalo SB, Eriksson JG, Sarkola T. Maternal obesity and gestational diabetes: Impact on arterial wall layer thickness and stiffness in early childhood - RADIEL study six-year follow-up. Atherosclerosis 2019.

(77) Sarkola T, Abadilla AA, Chahal N, Jaeggi E, McCrindle BW. Feasibility of very-high resolution ultrasound to assess elastic and muscular arterial wall morphology in adolescents attending an outpatient clinic for obesity and lipid abnormalities. Atherosclerosis 2011(2):610-615.

(78) Costa F, van Leeuwen MA, Daemen J, Diletti R, Kauer F, van Geuns RJ, et al. The Rotterdam Radial Access Research: Ultrasound-Based Radial Artery Evaluation for Diagnostic and Therapeutic Coronary Procedures. Circ Cardiovasc Interv 2016(2):e003129.

(79) Kaufman CL, Ouseph R, Blair B, Kutz JE, Tsai TM, Scheker LR, et al. Graft vasculopathy in clinical hand transplantation. Am J Transplant 2012(4):1004-1016.

(80) Latham GJ, Veneracion ML, Joffe DC, Bosenberg AT, Flack SH, Low DK. High-frequency micro-ultrasound for vascular access in young children--a feasibility study by the High-frequency UltraSound in Kids studY (HUSKY) group. Paediatr Anaesth 2013(6):529-535.

(81) Shen H, Zhou YJ, Liu YY, DU J, Liu XL, Yan ZX, et al. Assessment of early radial injury after transradial coronary intervention by high-resolution ultrasound biomicroscopy: innovative technology application. Chin Med J (Engl) 2012(19):3388-3392.

(82) Jaberi A, Muradali D, Marticorena RM, Dacouris N, Boutin A, Mulligan AM, et al. Arteriovenous fistulas for hemodialysis: application of high-frequency US to assess vein wall morphology for cannulation readiness. Radiology 2011(2):616-624.

(83) Hodges TC, Detmer PR, Dawson DL, Bergelin RO, Beach KW, Hatsukami TS, et al. Ultrasound determination of total arterial wall thickness. J Vasc Surg 1994(4):745-753.

(84) Skilton MR, Serusclat A, Sethu AH, Brun S, Bernard S, Balkau B, et al. Noninvasive measurement of carotid extra-media thickness: associations with cardiovascular risk factors and intima-media thickness. JACC Cardiovasc Imaging 2009(2):176-182.

(85) Falk E, Thim T, Kristensen IB. Atherosclerotic plaque, adventitia, perivascular fat, and carotid imaging. JACC Cardiovasc Imaging 2009(2):183-186.

(86) Cai TY, Sullivan TR, Ayer JG, Harmer JA, Leeder SR, Toelle BG, et al. Carotid extramedial thickness is associated with local arterial stiffness in children. J Hypertens 2016(1):109-115.

(87) Skilton MR, Serusclat A, Sethu AH, Brun S, Bernard S, Balkau B, et al. Noninvasive measurement of carotid extra-media thickness: associations with cardiovascular risk factors and intima-media thickness. JACC Cardiovasc Imaging 2009(2):176-182.

(88) Skilton MR, Sullivan TR, Ayer JG, Harmer JA, Toelle BG, Webb K, et al. Carotid extra-medial thickness in childhood: early life effects on the arterial adventitia. Atherosclerosis 2012(2):478-482.

(89) Rodriguez-Macias KA, Naessen T, Bergqvist D. Validation of in vivo noninvasive high-frequency ultrasonography of the arterial wall layers. Ultrasound in Medicine & Biology 2001(6):751-756.

(90) Akhter T, Wikstrom AK, Larsson M, Naessen T. Individual common carotid artery wall layer dimensions, but not carotid intima-media thickness, indicate increased cardiovascular risk in women with preeclampsia: an investigation using noninvasive high-frequency ultrasound. Circ Cardiovasc Imaging 2013(5):762-768.

(91) Akhter T, Larsson M, Wikstrom AK, Naessen T. Thicknesses of individual layers of artery wall indicate increased cardiovascular risk in severe pre-eclampsia. Ultrasound Obstet Gynecol 2014(6):675-680.

(92) Bohman H, Jonsson U, Von Knorring AL, Von Knorring L, Olsson G, Paaren A, et al. Thicker carotid intima layer, thinner media layer and higher intima/media ratio in women with recurrent depressive disorders: A pilot study using non-invasive high frequency ultrasound. World J Biol Psychiatry 2010(1):71-75.

(93) Dangardt F, Osika W, Volkmann R, Gan LM, Friberg P. Obese children show increased intimal wall thickness and decreased pulse wave velocity. Clin Physiol Funct Imaging 2008(5):287-293.

(94) Dangardt F, Charakida M, Chiesa S, Bhowruth D, Rapala A, Thurn D, et al. Intimal and medial arterial changes defined by ultra-high-frequency ultrasound: Response to changing risk factors in children with chronic kidney disease. PLoS One 2018(6):e0198547.

(95) Leonard D, Akhter T, Nordmark G, Ronnblom L, Naessen T. Increased carotid intima thickness and decreased media thickness in premenopausal women with systemic lupus erythematosus: an investigation by non-invasive high-frequency ultrasound. Scand J Rheumatol 2011(4):279-282.

(96) Myredal A, Gan LM, Osika W, Friberg P, Johansson M. Increased intima thickness of the radial artery in individuals with prehypertension and hypertension. Atherosclerosis 2010(1):147-151.

(97) Myredal A, Osika W, Li Ming G, Friberg P, Johansson M. Increased intima thickness of the radial artery in patients with coronary heart disease. Vasc Med 2010(1):33-37.

(98) Osika W, Dangardt F, Montgomery SM, Volkmann R, Gan LM, Friberg P. Sex differences in peripheral artery intima, media and intima media thickness in children and adolescents. Atherosclerosis 2009(1):172-177.

(99) Dangardt F, Chen Y, Berggren K, Osika W, Friberg P. Increased rate of arterial stiffening with obesity in adolescents: a five-year follow-up study. PLoS One 2013(2):e57454.

(100) Vatanen A, Sarkola T, Ojala TH, Turanlahti M, Jahnukainen T, Saarinen-Pihkala UM, et al. Radiotherapy-related arterial intima thickening and plaque formation in childhood cancer survivors detected with very-high resolution ultrasound during young adulthood. Pediatric Blood & Cancer 2015(11):2000-2006.

(101) Schmidt C, Wendelhag I. How can the variability in ultrasound measurement of intima-media thickness be reduced? Studies of interobserver variability in carotid and femoral arteries. Clin Physiol 1999(1):45-55.

(102) Touboul P-, Prati P, Scarabin P-, Adrai V, Thibout E, Ducimetière P. Use of monitoring software to improve the measurement of carotid wall thickness by B-mode imaging. J Hypertens 1992:S37-S41.

(103) Wendelhag I, Liang Q, Gustavsson T, Wikstrand J. A new automated computerized analyzing system simplifies readings and reduces the variability in ultrasound measurement of intima-media thickness. Stroke 1997(11):2195-2200.

(104) Selzer RH, Hodis HN, Kwong-Fu H, Mack WJ, Lee PL, Liu C-, et al. Evaluation of computerized edge tracking for quantifying intima-media thickness of the common carotid artery from B-mode ultrasound images. Atherosclerosis 1994(1):1-11.

(105) Stein JH, Korcarz CE, Mays ME, Douglas PS, Palta M, Zhang H, et al. A semiautomated ultrasound border detection program that facilitates clinical measurement of ultrasound carotid intima-media thickness. J Am Soc Echocardiogr 2005(3):244-251.

(106) Vermeersch SJ, Rietzschel ER, De Buyzere ML, Van Bortel LM, D'Asseler Y, Gillebert TC, et al. Validation of a new automated IMT measurement algorithm. J Hum Hypertens 2007(12):976-978.

(107) Ring M, Eriksson MJ, Jogestrand T, Caidahl K. Ultrasound measurements of carotid intima-media thickness by two semi-automated analysis systems. Clin Physiol Funct Imaging 2016(5):389-395.

(108) Molinari F, Zeng G, Suri JS. An integrated approach to computer-based automated tracing and its validation for 200 common carotid arterial wall ultrasound images: a new technique. J Ultrasound Med 2010(3):399-418.

(109) Liang Q, Wendelhag I, Wikstrand J, Gustavsson T. A multiscale dynamic programming procedure for boundary detection in ultrasonic artery images. IEEE Trans Med Imaging 2000(2):127-142.

(110) Peters SAE, Den Ruijter HM, Palmer MK, Grobbee DE, Crouse JR, O'Leary DH, et al. Manual or semi-automated edge detection of the maximal far wall common carotid intima-media thickness: A direct comparison. J Intern Med (GBR) 2012(3):247-256.

(111) Shenouda N, Proudfoot NA, Currie KD, Timmons BW, MacDonald MJ. Automated ultrasound edge-tracking software comparable to established semi-automated reference software for carotid intima-media thickness analysis. Clin Physiol Funct Imaging 2018(3):396-401.

(112) Mancia G, Fagard R, Narkiewicz K, Redon J, Zanchetti A, Bohm M, et al. 2013 ESH/ESC Practice Guidelines for the Management of Arterial Hypertension. Blood Press 2014(1):3-16.

(113) Weyand CM, Goronzy JJ. Medium- and large-vessel vasculitis. N Engl J Med 2003(2):160-169.

(114) Buttgereit F, Dejaco C, Matteson EL, Dasgupta B. Polymyalgia Rheumatica and Giant Cell Arteritis: A Systematic Review. JAMA 2016(22):2442-2458.

(115) Dejaco C, Duftner C, Buttgereit F, Matteson EL, Dasgupta B. The spectrum of giant cell arteritis and polymyalgia rheumatica: revisiting the concept of the disease. Rheumatology (Oxford) 2017(4):506-515.

(116) Franzen P, Sutinen S, von Knorring J. Giant cell arteritis and polymyalgia rheumatica in a region of Finland: an epidemiologic, clinical and pathologic study, 1984-1988. J Rheumatol 1992(2):273-276.

(117) Hunder GG. Epidemiology of giant-cell arteritis. Cleve Clin J Med 2002:SII79-82.

(118) Lee JL, Naguwa SM, Cheema GS, Gershwin ME. The geo-epidemiology of temporal (giant cell) arteritis. Clin Rev Allergy Immunol 2008(1-2):88-95.

(119) Gonzalez-Gay MA, Vazquez-Rodriguez TR, Lopez-Diaz MJ, Miranda-Filloy JA, Gonzalez-Juanatey C, Martin J, et al. Epidemiology of giant cell arteritis and polymyalgia rheumatica. Arthritis Rheum 2009(10):1454-1461.

(120) Weyand CM, Goronzy JJ. Giant-cell arteritis and polymyalgia rheumatica. N Engl J Med 2014(17):1653.

(121) Gonzalez-Gay MA, Matteson EL, Castaneda S. Polymyalgia rheumatica. Lancet 2017(10103):1700-1712.

(122) Weyand CM, Liao YJ, Goronzy JJ. The immunopathology of giant cell arteritis: diagnostic and therapeutic implications. J Neuroophthalmol 2012(3):259-265.

(123) Weyand CM, Goronzy JJ. Immune mechanisms in medium and large-vessel vasculitis. Nat Rev Rheumatol 2013(12):731-740.

(124) Deng J, Younge BR, Olshen RA, Goronzy JJ, Weyand CM. Th17 and Th1 T-cell responses in giant cell arteritis. Circulation 2010(7):906-915.

(125) Rodriguez-Pla A, Bosch-Gil JA, Rossello-Urgell J, Huguet-Redecilla P, Stone JH, Vilardell-Tarres M. Metalloproteinase-2 and -9 in giant cell arteritis: involvement in vascular remodeling. Circulation 2005(2):264-269.

(126) Weyand CM, Wagner AD, Björnsson J, Goronzy JJ. Correlation of the topographical arrangement and the functional pattern of tissue-infiltrating macrophages in giant cell arteritis. J Clin Invest 1996(7):1642-1649.

(127) Kaiser M, Weyand CM, Björnsson J, Goronzy JJ. Platelet-derived growth factor, intimal hyperplasia, and ischemic complications in giant cell arteritis. Arthritis Rheum 1998(4):623-633.

(128) Hayreh SS, Podhajsky PA, Zimmerman B. Ocular manifestations of giant cell arteritis. Am J Ophthalmol 1998(4):509-520.

(129) Aiello PD, Trautmann JC, McPhee TJ, Kunselman AR, Hunder GG. Visual prognosis in giant cell arteritis. Ophthalmology 1993(4):550-555.

(130) Allsop CJ, Gallagher PJ. Temporal artery biopsy in giant-cell arteritis. A reappraisal. Am J Surg Pathol 1981(4):317-323.

(131) Kent RB,3rd, Thomas L. Temporal artery biopsy. Am Surg 1990(1):16-21.

(132) Scott KR, Tse DT, Kronish JW. Temporal artery biopsy technique: a clinico-anatomical approach. Ophthalmic Surg 1991(9):519-525.

(133) Narvaez J, Bernad B, Roig-Vilaseca D, Garcia-Gomez C, Gomez-Vaquero C, Juanola X, et al. Influence of previous corticosteroid therapy on temporal artery biopsy yield in giant cell arteritis. Semin Arthritis Rheum 2007(1):13-19.

(134) Muratore F, Kermani TA, Crowson CS, Green AB, Salvarani C, Matteson EL, et al. Large-vessel giant cell arteritis: a cohort study. Rheumatology (Oxford) 2015(3):463-470.

(135) Mari B, Monteagudo M, Bustamante E, Perez J, Casanovas A, Jordana R, et al. Analysis of temporal artery biopsies in an 18-year period at a community hospital. Eur J Intern Med 2009(5):533-536.

(136) Gonzalez-Gay MA, Garcia-Porrua C, Llorca J, Gonzalez-Louzao C, Rodriguez-Ledo P. Biopsy-negative giant cell arteritis: clinical spectrum and predictive factors for positive temporal artery biopsy. Semin Arthritis Rheum 2001(4):249-256.

(137) Baldursson O, Steinsson K, Bjornsson J, Lie JT. Giant cell arteritis in Iceland. An epidemiologic and histopathologic analysis. Arthritis Rheum 1994(7):1007-1012.

(138) Rodriguez-Pla A, Rossello-Urgell J, Bosch-Gil JA, Huguet-Redecilla P, Vilardell-Tarres M. Proposal to decrease the number of negative temporal artery biopsies. Scand J Rheumatol 2007(2):111-118.

(139) Achkar AA, Lie JT, Hunder GG, O'Fallon WM, Gabriel SE. How does previous corticosteroid treatment affect the biopsy findings in giant cell (temporal) arteritis? Ann Intern Med 1994(12):987-992.

(140) Poller DN, van Wyk Q, Jeffrey MJ. The importance of skip lesions in temporal arteritis. J Clin Pathol 2000(2):137-139.

(141) Cristaudo AT, Mizumoto R, Hendahewa R. The impact of temporal artery biopsy on surgical practice. Annals of Medicine and Surgery 2016:47-51.

(142) Pinar YA, Govsa F. Anatomy of the superficial temporal artery and its branches: its importance for surgery. Surg Radiol Anat 2006(3):248-253.

(143) Yoon MK, Horton JC, McCulley TJ. Facial nerve injury: a complication of superficial temporal artery biopsy. Am J Ophthalmol 2011(2):251-255.e1.

(144) Schmidt WA, Kraft HE, Vorpahl K, Volker L, Gromnica-Ihle EJ. Color duplex ultrasonography in the diagnosis of temporal arteritis. N Engl J Med 1997(19):1336-1342.

(145) Aschwanden M, Daikeler T, Kesten F, Baldi T, Benz D, Tyndall A, et al. Temporal artery compression sign - a novel ultrasound finding for the diagnosis of giant cell arteritis. Ultraschall Med 2013(1):47-50.

(146) Black R, Roach D, Rischmueller M, Lester SL, Hill CL. The use of temporal artery ultrasound in the diagnosis of giant cell arteritis in routine practice. Int J Rheum Dis 2013(3):352-357.

(147) Bley TA, Reinhard M, Hauenstein C, Markl M, Warnatz K, Hetzel A, et al. Comparison of duplex sonography and high-resolution magnetic resonance imaging in the diagnosis of giant cell (temporal) arteritis. Arthritis Rheum 2008(8):2574-2578.

(148) Croft AP, Thompson N, Duddy MJ, Barton C, Khattak F, Mollan SP, et al. Cranial ultrasound for the diagnosis of giant cell arteritis. A retrospective cohort study. J R Coll Physicians Edinb 2015(4):268-272.

(149) Karahaliou M, Vaiopoulos G, Papaspyrou S, Kanakis MA, Revenas K, Sfikakis PP. Colour duplex sonography of temporal arteries before decision for biopsy: a prospective study in 55 patients with suspected giant cell arteritis. Arthritis Res Ther 2006(4):R116.

(150) LeSar CJ, Meier GH, DeMasi RJ, Sood J, Nelms CR, Carter KA, et al. The utility of color duplex ultrasonography in the diagnosis of temporal arteritis. J Vasc Surg 2002(6):1154-1160.

(151) Luqmani R, Lee E, Singh S, Gillett M, Schmidt WA, Bradburn M, et al. The Role of Ultrasound Compared to Biopsy of Temporal Arteries in the Diagnosis and Treatment of Giant Cell Arteritis (TABUL): a diagnostic accuracy and cost-effectiveness study. Health Technol Assess 2016(90):1-238.

(152) Maldini C, Depinay-Dhellemmes C, Tra TT, Chauveau M, Allanore Y, Gossec L, et al. Limited value of temporal artery ultrasonography examinations for diagnosis of giant cell arteritis: analysis of 77 subjects. J Rheumatol 2010(11):2326-2330.

(153) Muratore F, Boiardi L, Restuccia G, Macchioni P, Pazzola G, Nicolini A, et al. Comparison between colour duplex sonography findings and different histological patterns of temporal artery. Rheumatology (Oxford) 2013(12):2268-2274.

(154) Reinhard M, Schmidt D, Hetzel A. Color-coded sonography in suspected temporal arteritis-experiences after 83 cases. Rheumatol Int 2004(6):340-346.

(155) Schmidt D, Hetzel A, Reinhard M, Auw-Haedrich C. Comparison between color duplex ultrasonography and histology of the temporal artery in cranial arteritis (giant cell arteritis). Eur J Med Res 2003(1):1-7.

(156) Schmidt WA, Moller DE, Gromnica-Ihle E. Color duplex ultrasound of the temporal artery: replacement for biopsy in temporal arteritis. Ophthalmologica 2003(2):164-165.

(157) Salvarani C, Silingardi M, Ghirarduzzi A, Lo Scocco G, Macchioni P, Bajocchi G, et al. Is duplex ultrasonography useful for the diagnosis of giant-cell arteritis? Ann Intern Med 2002(4):232-238.

(158) Perez Lopez J, Solans Laque R, Bosch Gil JA, Molina Cateriano C, Huguet Redecilla P, Vilardell Tarres M. Colour-duplex ultrasonography of the temporal and ophthalmic arteries in the diagnosis and follow-up of giant cell arteritis. Clin Exp Rheumatol 2009(1 Suppl 52):S77-82.

(159) Karassa FB, Matsagas MI, Schmidt WA,Ioannidis JA. Meta-analysis: Test performance of ultrasonography for giant-cell arteritis. Annals of Internal Medicine 2005(5):359-369.

(160) Arida A, Kyprianou M, Kanakis M, Sfikakis PP. The diagnostic value of ultrasonography-derived edema of the temporal artery wall in giant cell arteritis: a second meta-analysis. BMC Musculoskeletal Disorders 2010:44-44.

(161) Ball EL, Walsh SR, Tang TY, Gohil R, Clarke JMF. Role of ultrasonography in the diagnosis of temporal arteritis. Br J Surg 2010(12):1765-1771.

(162) Rinagel M, Chatelus E, Jousse-Joulin S, Sibilia J, Gottenberg J, Chasset F, et al. Diagnostic performance of temporal artery ultrasound for the diagnosis of giant cell arteritis: a systematic review and meta-analysis of the literature. Autoimmunity Reviews 2019(1):56-61.

(163) Duftner C, Dejaco C, Sepriano A, Falzon L, Schmidt WA, Ramiro S. Imaging in diagnosis, outcome prediction and monitoring of large vessel vasculitis: a systematic literature review and meta-analysis informing the EULAR recommendations. RMD Open 2018(1):e000612-2017-000612.

(164) Hauenstein C, Reinhard M, Geiger J, Markl M, Hetzel A, Treszl A, et al. Effects of early corticosteroid treatment on magnetic resonance imaging and ultrasonography findings in giant cell arteritis. Rheumatology (Oxford) 2012(11):1999-2003.

(165) Monti S, Floris A, Ponte C, Schmidt WA, Diamantopoulos AP, Pereira C, et al. The use of ultrasound to assess giant cell arteritis: review of the current evidence and practical guide for the rheumatologist. Rheumatology (Oxford) 2018(2):227-235.

(166) Chrysidis S, Duftner C, Dejaco C, Schafer VS, Ramiro S, Carrara G, et al. Definitions and reliability assessment of elementary ultrasound lesions in giant cell arteritis: a study from the OMERACT Large Vessel Vasculitis Ultrasound Working Group. RMD Open 2018(1):e000598-2017-000598.

(167) Czihal M, Schrottle A, Baustel K, Lottspeich C, Dechant C, Treitl KM, et al. B-mode sonography wall thickness assessment of the temporal and axillary arteries

for the diagnosis of giant cell arteritis: a cohort study. Clin Exp Rheumatol 2017(1):128-133.

(168) Forster S, Tato F, Weiss M, Czihal M, Rominger A, Bartenstein P, et al. Patterns of extracranial involvement in newly diagnosed giant cell arteritis assessed by physical examination, colour coded duplex sonography and FDG-PET. Vasa 2011(3):219-227.

(169) Schmidt WA. Imaging in vasculitis. Best Pract Res Clin Rheumatol 2013(1):107-118.

(170) Schmidt WA. Ultrasound in the diagnosis and management of giant cell arteritis. Rheumatology (Oxford) 2018(s2):ii22-ii31.

(171) Nesher G, Breuer GS. Giant Cell Arteritis and Polymyalgia Rheumatica: 2016 Update. Rambam Maimonides Med J 2016(4):e0035.

(172) Dejaco C, Ramiro S, Duftner C, Besson FL, Bley TA, Blockmans D, et al. EULAR recommendations for the use of imaging in large vessel vasculitis in clinical practice. Ann Rheum Dis 2018(5):636-643.

(173) Roters S, Szurman P, Engels BF, Brunner R. The suitability of the ultrasound biomicroscope for establishing texture in giant cell arteritis. Br J Ophthalmol 2001(8):946-948.

(174) Vianna RN, Mansour M, Ozdal PC, Souza Filho JP, Bakalian S, Saraiva VS, et al. The role of ultrasound biomicroscopy in predicting the result of temporal artery biopsy in temporal arteritis patients: a preliminary study. Eur J Ophthalmol 2005(6):655-659.

(175) Avitabile T, Castiglione F, Bonfiglio V, Reibaldi M, Buccoliero D, La Bruna M, et al. The role of ultrasound biomicroscopy in the diagnosis of temporal arteritis. Acta Clin Croat 2012:31-35.

(176) Pattmoller M, Daas L, Viestenz A, Milioti G, Hasenfus A, Seitz B, et al. Ultrasound biomicroscopy in giant cell arteritis. Ophthalmologe 2018(2):150-153.

(177) Schneider CA, Rasband WS, Eliceiri KW. NIH Image to ImageJ: 25 years of image analysis. Nat Methods 2012(7):671-675.

(178) Alturkistani HA, Tashkandi FM, Mohammedsaleh ZM. Histological Stains: A Literature Review and Case Study. Glob J Health Sci 2015(3):72-79.

(179) Ciccia F, Ferrante A, Guggino G, Cavazza A, Salvarani C, Rizzo A. CD3 immunohistochemistry is helpful in the diagnosis of giant cell arteritis. Rheumatology (Oxford) 2018(8):1377-1380.

(180) Cavazza A, Muratore F, Boiardi L, Restuccia G, Pipitone N, Pazzola G, et al. Inflamed temporal artery: histologic findings in 354 biopsies, with clinical correlations. Am J Surg Pathol 2014(10):1360-1370.

(181) Brack A, Martinez-Taboada V, Stanson A, Goronzy JJ, Weyand CM. Disease pattern in cranial and large-vessel giant cell arteritis. Arthritis Rheum 1999(2):311-317.

(182) Braun J, Baraliakos X, Fruth M. The role of 18F-FDG positron emission tomography for the diagnosis of vasculitides. Clin Exp Rheumatol 2018(5):108-114.

(183) Caylor TL, Perkins A. Recognition and management of polymyalgia rheumatica and giant cell arteritis. Am Fam Physician 2013(10):676-684.

(184) Diaz VA, DeBroff BM, Sinard J. Comparison of histopathologic features, clinical symptoms, and erythrocyte sedimentation rates in biopsy-positive temporal arteritis. Ophthalmology 2005(7):1293-1298.

(185) Eberhardt RT, Dhadly M. Giant cell arteritis: diagnosis, management, and cardiovascular implications. Cardiol Rev 2007(2):55-61.

(186) Hayreh SS, Podhajsky PA, Raman R, Zimmerman B. Giant cell arteritis: validity and reliability of various diagnostic criteria. Am J Ophthalmol 1997(3):285-296.

(187) Koenigkam-Santos M, Sharma P, Kalb B, Oshinski JN, Weyand CM, Goronzy JJ, et al. Magnetic resonance angiography in extracranial giant cell arteritis. J Clin Rheumatol 2011(6):306-310.

(188) Salvarani C, Hunder GG. Giant cell arteritis with low erythrocyte sedimentation rate: frequency of occurence in a population-based study. Arthritis Rheum 2001(2):140-145.

(189) van der Geest KS, Abdulahad WH, Rutgers A, Horst G, Bijzet J, Arends S, et al. Serum markers associated with disease activity in giant cell arteritis and polymyalgia rheumatica. Rheumatology (Oxford) 2015(8):1397-1402.

(190) Bland JM, Altman DG. Statistical methods for assessing agreement between two methods of clinical measurement. Lancet 1986(8476):307-310.

(191) Hanley JA, McNeil BJ. A method of comparing the areas under receiver operating characteristic curves derived from the same cases. Radiology 1983(3):839-843.

(192) Freire CM, Ribeiro AL, Barbosa FB, Nogueira AI, de Almeida MC, Barbosa MM, et al. Comparison between automated and manual measurements of carotid intima-media thickness in clinical practice. Vasc Health Risk Manag 2009:811-817.

(193) Loizou CP, Pattichis CS, Pantziaris M, Tyllis T, Nicolaides A. Snakes based segmentation of the common carotid artery intima media. Med Biol Eng Comput 2007(1):35-49.

(194) Mancini GB, Abbott D, Kamimura C, Yeoh E. Validation of a new ultrasound method for the measurement of carotid artery intima medial thickness and plaque dimensions. Can J Cardiol 2004(13):1355-1359.

(195) Molinari F, Liboni W, Pavanelli E, Giustetto P, Badalamenti S, Suri JS. Accurate and automatic carotid plaque characterization in contrast enhanced 2-d ultrasound images. Conf Proc IEEE Eng Med Biol Soc 2007:335-338.

(196) Schmidt-Trucksäss A, Cheng D, Sandrock M, Schulte-Mönting J, Rauramaa R, Huonker M, et al. Computerized analysing system using the active contour in ultrasound measurement of carotid artery intima-media thickness. Clinical Physiology 2001(5):561-569.

(197) Faita F, Gemignani V, Bianchini E, Giannarelli C, Demi M. Real-time measurement system for the evaluation of the intima media thickness with a new edge detector. Conf Proc IEEE Eng Med Biol Soc 2006:715-718.

(198) Faita F, Gemignani V, Bianchini E, Giannarelli C, Ghiadoni L, Demi M. Real-time measurement system for evaluation of the carotid intima-media thickness with a robust edge operator. J Ultrasound Med 2008(9):1353-1361.

(199) Loizou CP, Pattichis CS, Pantziaris M, Tyllis T, Nicolaides A. Quality evaluation of ultrasound imaging in the carotid artery based on normalization and speckle reduction filtering. Med Biol Eng Comput 2006(5):414-426.

(200) Loizou CP, Pattichis CS, Christodoulou CI, Istepanian RS, Pantziaris M, Nicolaides A. Comparative evaluation of despeckle filtering in ultrasound imaging of the carotid artery. IEEE Trans Ultrason Ferroelectr Freq Control 2005(10):1653-1669.

(201) Loizou CP, Pattichis CS, Nicolaides AN, Pantziaris M. Manual and automated media and intima thickness measurements of the common carotid artery. IEEE Trans Ultrason Ferroelectr Freq Control 2009(5):983-994.

(202) Rousson V, Gasser T, Seifert B. Assessing intrarater, interrater and test-retest reliability of continuous measurements. Stat Med 2002(22):3431-3446.

(203) Stergiotou I, Crispi F, Valenzuela-Alcaraz B, Cruz-Lemini M, Bijnens B, Gratacos E. Aortic and carotid intima-media thickness in term small-for-gestational-Age newborns and relationship with prenatal signs of severity. Ultrasound Obstet Gynecol 2014(6):625-631.

(204) Schubert U, Müller M, Abdul-Khaliq H, Norman M, Bonamy A-E. Relative intima-media thickening after preterm birth. Acta Paediatr Int J Paediatr 2013(10):965-969.

(205) Atabek ME, Çagan HH, Eklioglu BS, Oran B. Absence of increase in carotid artery Intima-Media thickness in infants of diabetic mothers. JCRPE J Clin Res Pediatr Endocrinol 2011(3):144-148.

(206) Hondappanavar A, Sodhi KS, Dutta S, Saxena AK, Khandelwal N. Quantitative ultrasound measurement of intima-media thickness of abdominal aorta and common carotid arteries in normal term newborns. Pediatr Cardiol 2013(2):364-369.

(207) Ikari Y, McManus BM, Kenyon J, Schwartz SM. Neonatal intima formation in the human coronary artery. Arterioscler Thromb Vasc Biol 1999(9):2036-2040.

(208) van Meurs-van Woezik H, Klein HW, Markus-Silvis L, Krediet P. Comparison of the growth of the tunica media of the ascending aorta, aortic isthmus and descending aorta in infants and children. J Anat 1983(Pt 2):273-281.

(209) Vlachopoulos C, Georgakopoulos C, Koutagiar I, Tousoulis D. Diagnostic modalities in peripheral artery disease. Curr Opin Pharmacol 2018:68-76.